Examining the self-correction of brain malformations in pre-metamorphic *Xenopus laevis*

An honors thesis

submitted by

Maura J. Barry

In partial fulfillment of the requirements

for the degree of

Bachelor of Science

in

Biology

TUFTS UNIVERSITY

School of Arts and Sciences

May 2019

Advisor: Kelly A. McLaughlin, Ph.D.

ABSTRACT

Craniofacial deformities are common developmental defects across all vertebrate species, which can be caused by genetic factors, environmental factors, or a combination of both. Typically, in humans, these birth defects cannot be treated, or the only form of treatment is an expensive and invasive surgery. Thus, there is a critical need to study not just the causes of craniofacial defects in vertebrate model systems, but also potential resolutions and treatments for these craniofacial defects. Previous work by the McLaughlin lab determined that *Xenopus laevis* tadpoles with craniofacial deformities improve their overall morphology prior to metamorphosis by remodeling malformed craniofacial tissues, such as cartilage and eye tissue. In these works, we show that this self-correction process also includes the remodeling and repair of brain tissue. To elucidate the mechanism by which this self-correction process occurs, brain tissue differentiation and cerebrospinal fluid flow were examined in control and malformed brains. We found that both Pax7 spatial patterning and cerebrospinal fluid flow are altered in brains with malformations induced via teratogen exposure during embryogenesis but improve over time along with the overall morphology of the brains. In addition, the genetic factors involved in the self-correction of abnormal brain tissue were studied through RNA-seq and RT-qPCR procedures. The RNA-seq experiment identified prolactin hormone involvement in the self-correction mechanism that occurs in *Xenopus laevis* tadpoles prior to metamorphosis. Additional RT-qPCR experiments confirmed differential *prolactin.2.S* regulation in tadpole brain tissues undergoing self-correction and revealed differential expression of various *mmp*

genes. Furthermore, we found prolactin causes upregulation of *mmp* genes in brain tissue, predominantly *mmp1*. This suggests that the differential *mmp* expression that occurs in brains undergoing remodeling and repair is at least partially due to prolactin signaling. This implication that prolactin hormone and upregulation in *mmp* expression are directly involved in the self-correction process that occurs in pre-metamorphic *Xenopus laevis* tadpoles brings us one step closer to elucidating this exact mechanism and forming a more effective treatment for debilitating craniofacial deformities in humans.

ACKNOWLEDGEMENTS

I am so incredibly grateful to have had the opportunity to conduct research in the McLaughlin lab these past two years. Working in a developmental biology lab has been instrumental in my undergraduate education and has changed my college experience for the better. I remember frantically emailing Mike Grossi at the end of my sophomore year asking him if he knew of any lab positions open in the biology department at Tufts, as I was eager to get involved in research. A few weeks later, I received an email from him telling me that there was just one lab with an opening for the summer. I feel so lucky that it turned out to be the McLaughlin lab because I truly could not have found a better place to work on this campus. I cannot thank Dr. Kelly McLaughlin enough for allowing me to conduct research and pursue a senior thesis. Kelly, the support that you give the researchers in your lab is incredible. You never forget to celebrate a birthday and always bring everyone's favorite snacks to lab meetings! Thank you for your kindness and for challenging me in my learning. I never would have known how much I enjoy conducting research if I hadn't worked in your lab, so I really appreciate everything you've done for me!

Next, I want to thank Kayli Pinet, who has been the most amazing and supportive mentor. Thank you for answering my millions of questions and emails over the years and for teaching me every lab technique I know! I really appreciate your willingness to edit every one of my papers, posters, and especially this thesis. I wouldn't have been able to do any of it without you, and your help has allowed me to grow as a scientist. I can't express my gratitude enough! Congratulations on

completing your dissertation and becoming a doctor! You are such an amazing scientist and I know you will do great things in the next chapter of your life.

I would like to thank the other members of the McLaughlin lab who I have had the pleasure of working with during my time here: Kyle Jewhurst, Adam Bayless, Dan Lukason, Renee Chiu, Hannah Harris, Henna Tiwary and Zachary Rosh. Kyle, Adam, Dan and Hannah, thank you all for answering any questions I had and for your company while working in the lab! Renee, Henna and Zach, thanks for always being friendly faces in the lab and around campus! It was such a pleasure working and collaborating with all of you. I also want to thank Dr. Susan Koegel for being a member of my thesis committee and giving excellent advice concerning my research pursuits, as well as Dr. Benjmain Wolfe, who has been such a caring and supportive advisor for me in the biology department.

Thank you to Anne Moore of the Tufts Summer Scholars Program for allowing me to pursue a ten-week research project in the McLaughlin lab last summer. The work I did for the Summer Scholars Program was critical for my thesis, and it gave me the opportunity to present my findings at two research symposiums.

Finally, I want to thank my parents and my brother Kevin for their love and support! Although they don't know too much about biology (or science in general), they are always willing to listen to me talk about my tadpoles!

TABLE OF CONTENTS

LIST OF FIGURES AND TABLES

Chapter One

Chapter Two

LIST OF ABBREVIATIONS

AP	Anterior-posterior
BMP	Bone morphogenetic protein
CF	Craniofacial
CLP	Cleft lip/palate
CSF	Cerebrospinal fluid
CNCC	Cranial neural crest cell
EGTA	Ethylene glycol-bi(β-aminoethyl ether)-N,N,N',N'-tetraacetic acid
EtOH	Ethanol
FASD	Fetal alcohol spectrum disorder
FB	Forebrain
HB	Hindbrain
ISH	*in situ* hybridization
ICI 118,551	Imperial Chemical Industries 118,551 hydrochloric acid
KW	Kruskal Wallis
LMS	Lenz microphthalmia syndrome
LR	Left-right
MB	Midbrain
MEMFA	MOPS, EGTA, Magnesium sulfate, and Formaldehyde
MLK	Mixed-lineage kinase
MMP	Matrix metalloproteinase
MMR	Marc's modified Ringer's solutions
MO	Morpholino
NBT	Nitroblue tetrazolium
NCC	Neural crest cell
NF	Nieuwkoop and Faber
PBS	Phosphate buffered saline
PBTr	Phosphate buffered saline with Tris
pH	Potential of hydrogen

PRL	Prolactin
PRLR	Prolactin receptor
PM	Pergolide mesylate
RNA	Ribonucleic acid
RNAseq	Whole-transcriptome shotgun sequencing
RT-qPCR	Quantitative polymerase chain reaction
ThioHCl	Thioridazine hydrochloric acid
WT	Wild-type
xMLTK	Xenopus MLK-like mitogen-activated protein triple kinase

Examining the self-correction of brain malformation in pre-metamorphic *Xenopus laevis*

CHAPTER ONE

Introduction

Developmental biology: organ development, remodeling, regeneration, and repair

Developmental biologists study the various signaling pathways and cell interactions that mediate the creation of functional organs from individual cells. The creation of organs during development is not a completely understood biological process, and there is still much to learn about how organisms begin as individual cells with identical DNA and end with differentiated cells with specific roles within complex tissue structures. However, we do know that cells differentiate based on highly regulated and well conserved gene regulatory networks as well as biophysical factors, which create the different organs and tissues necessary for life in an organism (Simoes-Costa and Bronner, 2015; Friston et al., 2015; Van Otterloo et al., 2013).

The McLaughlin lab at Tufts University is a developmental biology lab that focuses on vertebrate organ development, remodeling, regeneration, and repair. One of the overarching goals of the McLaughlin lab is to better understand how malformed tissues can be remodeled to improve organ function, which could lead to the discovery of novel medical treatments for correcting human diseases and deformities. Here, we investigate the mechanisms that control the remodeling of malformed tissues by utilizing the amphibian (frog) model system, *Xenopus laevis*.

Craniofacial development in vertebrates

Craniofacial defects are caused by disruptions in craniofacial development, which is very complex and strictly regulated process in vertebrates. The

development of the vertebrate head involves the formation of the vertebral column, brain, sensory organs, jaws, nerves, blood vessels, skeletal muscles, and cartilage (Van Otterloo et al., 2016). A complex development such as this leaves a lot of room for error. Signaling pathways and gene products regulate the formation of craniofacial tissues and organs and any disruptions in these pathways could induce craniofacial defects. For example, a study in mice showed that absence of either the G-coupled endothelin- receptor (ET_A) or endothelin-1 (ET-1) in the development of neural crest cells results in numerous craniofacial defects (Clouthier et al., 2000). In organisms lacking ET_A and/or ET-1, it appears that migration of the neural crest cells in the head of the embryos is normal, but there is either a reduction or complete absence of certain transcription factors (Clouthier et al., 2000). This leads to retarded arch growth, defects in proper differentiation, and mesenchymal cell apoptosis (Clouthier et al., 2000).

Frequently, craniofacial abnormalities are linked to alterations in migration or differentiation of cranial neural crest cells (Liu, 2016). Neural crest cells are a multipotent cell population central and unique to the evolution and development of the head in vertebrates (Van Otterloo et al., 2016). Neural crest cells originate at the dorsal junction between the neuroepithelium and the surface ectoderm, then cranial neural crest cells (CNCCs) migrate anteriorly and form distinct structures of the face (Hu et al., 2015). After CNCCs complete their migration into the facial primordia, a process of growth and patterning begins that causes the CNCCs to differentiate and give rise to craniofacial tissues, neurons, and muscles (Van Otterloo et al., 2016). The neural crest cells interact with the surrounding

mesoderm, endoderm and ectoderm to form these facial structures as well as the craniofacial cartilage and/or skeleton (Van Otterloo et al., 2016). Therefore, any disruptions in the migration of neural crest cells or the processes that lead to the formation of the vertebrate head can cause craniofacial abnormalities.

Craniofacial development is also a highly conserved process among vertebrate species, which means that research on vertebrate animal models can mimic processes in human beings (Van Otterloo et al., 2016; Dubey and Saint-Jeannet, 2017; Liu, 2016; Achilleos and Trainor, 2015; Goodwin et al., 2015; Square et al., 2015) (Figure 1.1). This also implies that vertebrates are generally susceptible to the same craniofacial defect-inducing teratogens, genetic disorders, and biophysical pressures (Van Otterloo et al., 2016, Dubey and Saint-Jeannet, 2017, Marrs et al., 2010). A single teratogen, such as ethanol, can even result in similar abnormal craniofacial phenotypes across several vertebrate species (e.g. humans, mice, fish, and frogs) (Shi et al., 2014; Guizzetti, 2015; Kumar et al., 2010; Kot-Leibovich and Fainsod, 2009a; Yelin et al., 2007). Thus, a better understanding of craniofacial development through research on animal models helps clarify how certain malformations arise and may ultimately inform the development of medical treatments.

Abundance of craniofacial abnormalities

Craniofacial deformities are common developmental defects across all vertebrate species, and they can be caused by genetic factors, environmental factors, or a combination of both. Craniofacial (CF) defects in humans, like cleft

lip and cleft palate, are among the most common birth defects in the world. In the United States, about 2,650 babies are born with cleft palate, and 4,440 babies are born with cleft lip (with or without cleft palate) (Parker et al., 2010). These defects can be devastating for patients and families, as they can result in impairment of function and require lifelong care (Lui, 2016). Craniofacial deformities can also involve malformed brain tissue and compromised behavioral functions, as is seen with Fetal Alcohol Spectrum Disorders (FASDs), which are a group of conditions that can occur in an individual whose mother consumed alcohol during pregnancy (Guizzetti, 2015). Worldwide prevalence of FASD varies, ranging from 1.06 to 113.22 per 1000 people (Reid et al., 2018). The symptoms associated with FASD can include facial deformities, such as microcephaly (small head size), ocular anomalies (usually wide-set eyes), lack of philtrum (ridge between the nose and upper lip), congenital heart defects, and malformed brain tissue, leading to intellectual defects (Shi et al., 2014; Parker et al., 2010). Alcohol causes neural crest apoptosis, perturbation of neural crest migration, and deterioration of cartilage (Shi et al., 2014). Furthermore, any FASD-associated brain defects are likely to cause difficulties in learning, memory, and attention, as the overall brain size is usually smaller in these cases, with a malformed corpus callosum and cerebellum (Guizzetti, 2015). The higher the concentration of alcohol exposure during embryogenesis, the more severe the defects (Guizzetti, 2015; Shi et al., 2014).

Craniofacial deformities may be caused by random genetic mutations, or environmental factors such as ethanol or folic acid deficiency (Carpeta et al., 2018, Webster et al., 1983, Christensen et al., 2018). For many facial deformities, surgery

is the only effective form of treatment, which is not only dangerous but expensive and intrusive. Many craniofacial deformities which include brain defects, like FASDs, have even fewer treatment options. Therefore, there is a great need for an improved, more effective way to treat facial defects and/or malformed brain tissue. New treatments that could direct the correction of birth defects would drastically change the lives of thousands of people, and help them to lead healthy, happy lives.

Xenopus laevis as a model organism for craniofacial tissue remodeling

Xenopus laevis, commonly known as the African clawed frog, is a tractable model system for studying craniofacial deformities and tissue remodeling because it is easily observed, amenable to manipulation during development, a fast developer, and is a vertebrate animal (Figure 1.2). Therefore, *Xenopus laevis'* craniofacial development is very similar to that of human beings, and the findings of studies with these animals can be related to humans. In addition, *Xenopus laevis* has a large clutch size, external development, and relatively large embryos, which is helpful for imaging (Figure 1.2).

Perhaps the most useful and intriguing aspect of *Xenopus laevis,* is that larvae with malformed craniofacial tissues are able to partially or entirely correct themselves prior to metamorphosis (Vandenberg et al., 2012). A study by Vandenberg *et al.* showed that the knockdown of the H+-V-ATPase channel in *Xenopus laevis* altered membrane potential, pH and gene expression, causing craniofacial abnormalities (Vandenberg, Morrie & Adams, 2011). Surprisingly, it was observed that over time, these defects normalized to become similar to control

groups (Vandenberg et al., 2012). No other vertebrate model system has been shown to be able to spontaneously correct these kinds of developmental defects. Although the ability for abnormal tissues in tadpoles to self-correct was documented by Vandenberg *et al.*, how these tissues were able to become more like normal animals remained a mystery.

The McLaughlin Lab begun to elucidate the underlying mechanisms that direct the self-correction of malformed tissues in the heads of tadpoles. It was determined that craniofacial deformities could be induced in *Xenopus laevis* pre-metamorphic tadpoles by exposing them to various chemical treatments during neurulation (see Figure 1.2 for reference), stages 14-25 (Nieuwkoop & Faber, 1994). ICI 118,551 HCl, thioridazine HCl, and ethanol were used for these exposures. ICI 118,551 HCl is a β_2-adrenoceptor antagonist and caused abnormal trapezoidal-shaped head phenotypes in tadpoles due to the absence of anterior mandibular cartilage elements (Figure 1.3) (Smith et al., 1987). Thioridazine HCl is a dopamine receptor antagonist, which was found to cause a square head phenotype, misshapen eyes, and hyper-pigmentation in tadpoles that were exposed to the drug during neurulation (Figure 1.3) (Sachlos et al., 2012). Ethanol, a retinoic acid signaling antagonist, produced a very similar phenotype in tadpoles as a child with severe Fetal Alcohol Syndrome: microcephaly and ocular deformities (Figure 1.3) (Kot-Leibovich and Fainsod, 2009b; Shi et al., 2014). The McLaughlin lab went on to show that the overall craniofacial morphology of the thioridazine HCl and ethanol treatment groups improved prior to metamorphosis, while the abnormal

morphology of tadpoles in the ICI 118,551 HCl treatment group remained unchanged.

Elucidating the mechanism by which this self-correction occurs in pre-metamorphic tadpoles is a current goal of the McLaughlin lab. Disruptions in the processes of the brain are often related to facial malformations, as facial formation seems to be related to healthy brain formation (Marcucio et al., 2015; Adameyko and Fried, 2016; Hu et al., 2015). Furthermore, the brain is required for normal muscle and nerve development in *Xenopus laevis*, making it likely that the presence of the brain, or signals from the brain, have an important role in normal craniofacial development (Herrera-Rincon and Levin, 2018). Thus, a study investigating the role of the brain in this self-correction process in *X. laevis* larvae was necessary.

Scope of Thesis

The aim of this thesis is to investigate the mechanisms of craniofacial tissue repair and remodeling in *Xenopus laevis*, focusing specifically on brain tissue in pre-metamorphic larvae. The overall goal of this research is to better understand the innate normalization of malformed brains in *X. laevis* tadpoles, in order to elucidate the mechanism by which these organisms self-correct brain and head deformities. This could lead to the development of improved treatment methods for human craniofacial birth defects.

Summary of Chapters

In Chapter 2, we examine the repair and remodeling of brain abnormalities in pre-metamorphic *Xenopus laevis* tadpoles. We begin by characterizing the brain phenotypes at early and late pre-metamorphic stages, in order to determine and characterize how well these animals can resolve brain abnormalities. Then, through various indicators, we found that the remodeling and repair of malformed brain tissues in these animals involved increased cell proliferation and altered matrix-metalloproteinase regulation. For this work, I examined cell differentiation through Pax7 protein expression patterns and cerebrospinal fluid flow across pre-metamorphic stages during the self-correction period. This work will be submitted for publication to Developmental Dynamics.

Chapter 3 discusses the significance and broader impact of the conclusions made from this honors thesis work, as well as future directions for the project. Also, an Appendix is included which details an additional set of preliminary experiments for characterizing the spatial patterning of another brain patterning marker, tyrosine hydroxylase, in the brains of *X. laevis* tadpoles with malformed tissues during pre-metamorphic life stages.

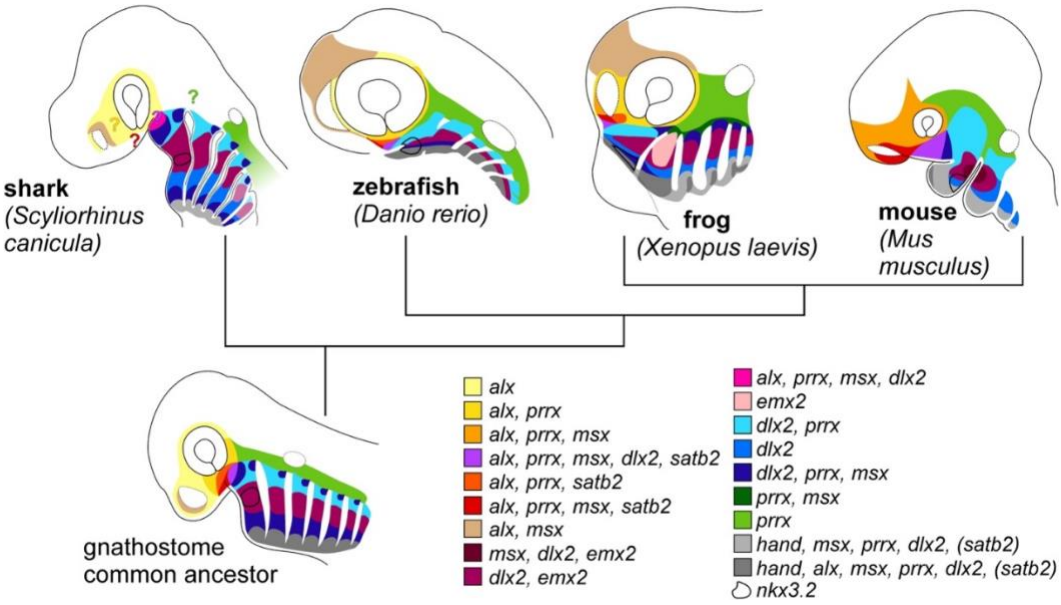

Figure 1.1 Mesodermal gene expression maps of larval vertebrate head skeletons highlights the conservation of craniofacial gene patterning across vertebrates. The larval head of a representative shark (*Scyliorhinus canicula*), ray-finned fish (zebrafish; *Danio rerio*), frog (*Xenopus laevis*), and mouse (*Mus musculus*) are shown with combinational transcription factors mapped out in multiple colors. The heads are arranged with anterior to the left. A hypothetical expression map of a gnathostome common ancestor is represented at the bottom-left of the figure based on published expression data. Craniofacial development is shown to be highly conserved among different vertebrate species, as is shown by the similar color patterns across the organisms. Figure taken from Square et al., 2015 (Fig. 4).

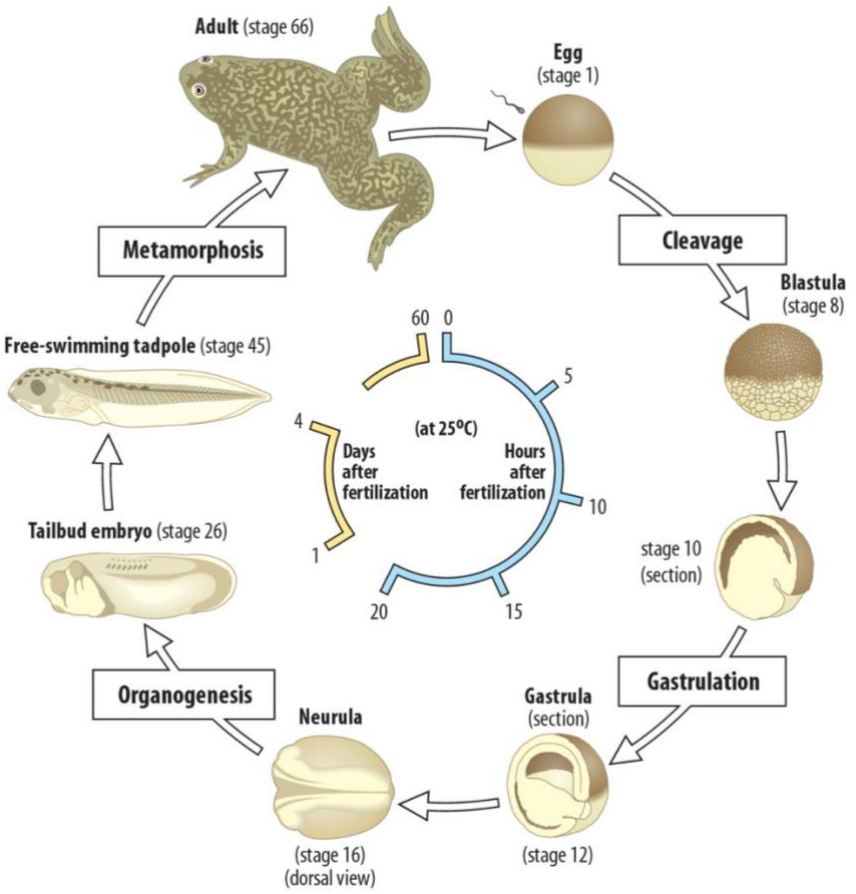

Figure 1.2 *Xenopus laevis* life cycle. There are several distinct and important pathways that *Xenopus laevis* undergo after fertilization and prior to metamorphosis, which is when tadpoles develop into mature frogs. During cleavage, the overall volume of the egg stays the same, but it is divided into tens of thousands of cells. Gastrulation indicates the formation of the germ layers, and neurulation is the formation of the neural tube. During organogenesis, the embryo elongates into its typical tadpole form, and neural crest cells give rise to neurons, cartilage, muscles and other structures through cell differentiation and morphogenesis. Figure from http://www.mun.ca/biology/desmid/brian/BIOL3530.html.

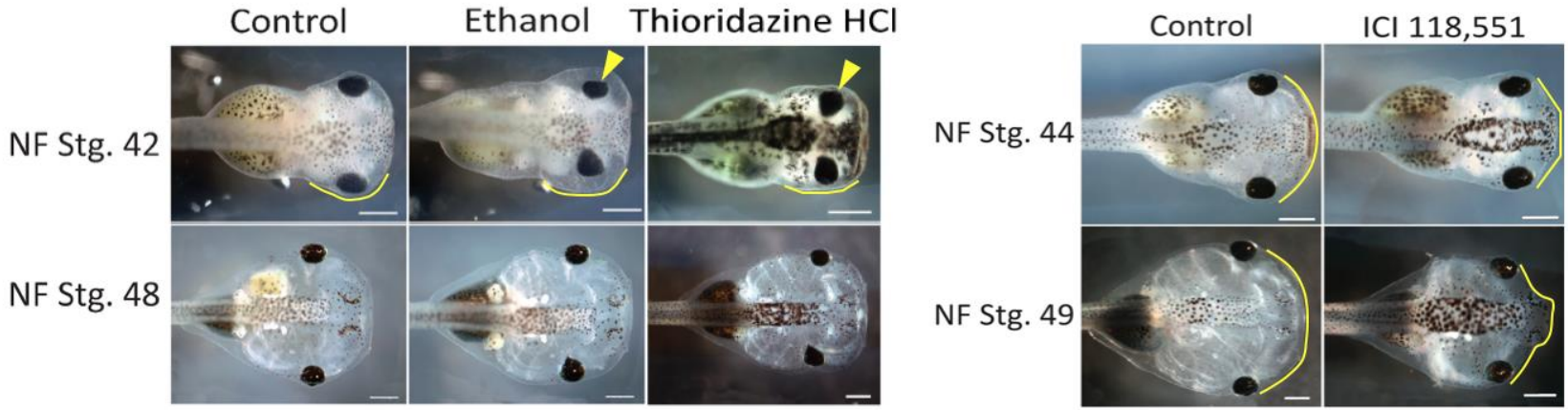

Figure 1.3 *Xenopus laevis* corrects ethanol and thioridazine HCl induced craniofacial deformities, but cannot correct ICI 118,551 induced craniofacial

Figure 1.3 *Xenopus laevis* corrects ethanol and thioridazine HCl induced craniofacial deformities, but cannot correct ICI 118,551 induced craniofacial deformities

Xenopus laevis tadpoles have the unique ability to self-correct craniofacial defects over time, as was first noted in the Vandenberg et al. paper in 2012, suggesting a tissue remodeling process. The McLaughlin Lab exposed pre-metamorphic tadpoles to three different teratogens: ethanol, an antagonist of the Retinoic Acid signaling pathway, Thioridazine HCl, a dopamine inhibitor, and ICI 118,551, a beta-adrenergic antagonist. Ethanol and thioridazine exposures cause abnormal craniofacial morphology that can fix over time (from stage 42 to 48 in these images), but abnormal phenotypes seen with beta blocker, ICI, cannot be fixed due to an absence of cartilage. The yellow borders and arrows highlight malformations in the treated tadpole heads as compared to the control heads. The arrows point to malformed or "cone-shaped" eyes. At stage 49, only ICI tadpoles still have an irregular, trapezoidal-shaped head. Photo credit to Kaylinnette Pinet. Scale bar = 500μm.

CHAPTER TWO

Repair and Remodeling of Brain Abnormalities in Pre-Metamorphic *Xenopus laevis* Tadpoles Through Increased Cell Proliferation and Altered Matrix-metalloproteinase regulation.

Kaylinnette Pinet[1], Maura Barry[1], Zachary Rosh[1], Brian Leung[1], and Kelly A. McLaughlin[1*]

[1]Allen Discovery Center at Tufts University

[*]Corresponding Author:

Dr. Kelly A. McLaughlin

Biology Department,

Center for Regenerative and Developmental Biology,

Allen Discovery Center at Tufts University,

Tufts University

200 Boston Avenue, Suite 4700

Medford, MA 02155-4243

Phone: +1 617 627 4154

Email: kelly.mclaughlin@tufts.edu

Key words: *Xenopus laevis*; Brain; Tissue remodeling; Tissue repair; Prolactin; Morphology

Data and writing contributions to the chapter: K.P. contributed to experimental design, data collection, data analysis, and writing. M.B., Z.R., and B.L. assisted with data collection and writing. K.M. contributed to experimental design and writing.

This chapter will be submitted to *Development Dynamics*.

Abstract

Background

Amongst vertebrates, craniofacial birth defects are often associated with malformed brain tissue. We previously confirmed that defects observed in *Xenopus laevis* larvae involving eye and craniofacial cartilaginous tissues can improve via tissue remodeling during pre-metamorphic stages. Here we characterize the underlying brain defects associated with the more external craniofacial defects seen after short-term pharmacological exposures to ethanol, thioridazine HCl, and ICI 118,551 HCl during neurulation. We also investigate the potential repair and remodeling of abnormal brain tissue prior to metamorphosis.

Results

We determined that the repair and remodeling of abnormal brain tissue in pre-metamorphic tadpoles occurs in conjunction with the correction of malformed craniofacial features. Furthermore, dysmorphic brains undergoing repair and remodeling show elevated prolactin and matrix metalloproteinase (*mmp1, mmp13*, or *mmp7*) gene expression, as well as significant increases in brain cell proliferation.

Conclusions

We reveal that *Xenopus laevis* larvae can correct abnormal brain tissue via a tissue remodeling and repair mechanism prior to the onset of metamorphosis. These results also suggest that prolactin signaling, differential *mmp* gene regulation, and cell proliferation play a role in the remodeling and repair of malformed brain tissue in *Xenopus laevis* pre-metamorphic tadpoles.

Introduction

Vertebrate animals have a tightly linked developmental regiment for craniofacial and brain tissue development. This connection is largely due to the close spatial relationship between neuronal progenitor cells and cranial neural crest cells (CNCCs) and their interdependent gene regulatory networks. As a result, craniofacial birth anomalies amongst vertebrates are often associated with malformed brain tissue (Marcucio et al., 2015). While facial abnormalities are the more apparent and salient aspects of these disorders, underneath lie neural deformities with equal if not greater significance. For example, fetal alcohol spectrum disorder (FASD), cleft lip/palate (CLP), and Lenz microphthalmia syndrome (LMS) are all characterized by abnormal or malformed craniofacial features, as well as mild to severe effects on cognition due to brain abnormalities (Kodituwakku and Kodituwakku, 2014; Roberts et al., 2012; Patel et al., 2018). Given that there are little to no treatment options for developmental brain abnormalities, it is imperative to investigate instances of craniofacial (CF) and brain repair and remodeling in animal models.

We previously confirmed that gross structural malformations in *Xenopus laevis* larvae, such as abnormal eyes and irregular cartilaginous tissues, caused by exposure to various teratogens during neurulation, self-correct prior to metamorphosis via tissue remodeling (Pinet et al., 2019). Here we investigate whether *X. laevis* pre-metamorphic tadpoles also self-correct the brain phenotypes associated with ethanol, thioridazine, and ICI 118,551-induced craniofacial defects. Gross brain morphology, cell proliferation, apoptosis, cerebrospinal fluid flow, and

tissue patterning were examined in these experimental organisms, as well as wild-type animals, throughout pre-metamorphic stages. In some or all the experimental groups, we observed atypical brain morphology, cell proliferation, tissue patterning, and cerebrospinal fluid flow at early pre-metamorphic stages. However, prior to entering metamorphic life stages many of the abnormal brain phenotypes partially or completely normalized, suggesting that these animals experienced an innate tissue remodeling and repair event in response to their pharmacologically-induced neural tissue malformations.

Neural tissue remodeling is a relatively new concept, with substantial implications for brain plasticity and cognitive capacity. Research studies focused on neural tissue remodeling (neural plasticity) have found that it occurs not only throughout neural development in juvenile animals, but also during adulthood (Gregg et al., 2007; Song and Dityatev, 2018; Zhornitsky et al., 2013; Shingo et al., 2003). Furthermore, there is evidence that endocrine (prolactin and growth hormone) signaling-dependent extracellular remodeling by matrix metalloproteinases (MMPs) is critical to neural plasticity in juvenile and adult animals (Gregg et al., 2007; Parhar, 2003; Costanza and Pedotti, 2016). Studies on mammals and amphibians have shown that prolactin signaling regulates the expression of certain matrix metalloproteinases (MMPs) (Jung et al., 2004; Philips and McFadden, 2004). MMPs are the major enzymes responsible for degrading proteins within the extracellular matrix (Jabłońska-Trypuć et al., 2016). Subsequently, MMPs and their inhibitors play a major role in physiological and

pathological tissue remodeling processes, such as morphogenesis, angiogenesis, and cancer metastasis (Beurden and Hoff, 2005).

To gain a better understanding of the underlying molecular mechanisms mediating the remodeling and repair of malformed brain tissues in pre-metamorphic *X. laevis* specimen, we applied a global RNAseq-based gene expression analysis on brain tissue isolated from wild-type controls and tadpoles with self-correcting brain phenotypes. This RNAseq analysis revealed an upregulation of remodeling factors, such as *gnrh2*, *prolactin.2*, and *mmp7* in the brain tissue of animals just prior to or during the repair and remodeling period. We then utilized RT-qPCR to confirm that the repair and remodeling of abnormal brain tissue in pre-metamorphic tadpoles coincides with differential expression of *prl.2* and *mmp7*, as well as *mmp1* and *mmp13*, relative to wild-type brain tissue. MMP7 is a matrilysin enzyme, while MMP1 and MMP13 are both interstitial collagenases that have previously been shown to be regulated by prolactin signaling in *X. laevis* cell cultures (Maeda et al., 1995; Quillard et al., 2014; Yueh et al., 2018; Jung et al., 2004).

To test the effect of Prolactin.2 on *mmp1, mmp13, and mmp7* expression within brain tissue, *in vivo*, we experimentally altered Prolactin.2 signaling in wild-type pre-metamorphic tadpoles. We found a strong and direct correlation between altered Prolactin.2 signaling and the differential expression of *mmp1* in pre-metamorphic *X. laevis* tadpole brain tissue. While inhibiting or inducing prolactin signaling in wild-type controls was not sufficient to fully recapitulate the differential regulation of *Prl.2, mmp1, mmp13, and mmp7* seen in brain tissue

undergoing remodeling and repair, these data suggest that prolactin signaling is integral to brain growth and development in *Xenopus* larvae. Furthermore, these findings strongly suggest that MMPs (i.e., MMP1, MMP13, and MMP7) and a multifaceted endocrine hormone signaling cascade play a role in the correction of malformed brain tissue and maintenance of normal brain morphology in *X. laevis* pre-metamorphic tadpoles. However, further studies are needed to identify additional directive signaling pathways and molecules responsible for the normalization of malformed brain tissue in these animals. Once these remodeling and repair mechanisms are more well-understood, they will likely inspire future translational research and novel medical therapies.

Results

Abnormal brain tissue morphology improves during pre-metamorphic stages

In order to examine whether teratogen-induced brain deformities normalized during pre-metamorphic stages in *Xenopus laevis,* we had to observe brain phenotypes at early and late pre-metamorphic stages. While the effect of thioridazine or ICI 118,551 exposure during neurulation on brain morphology has not been previously described in *X. laevis*, various studies have demonstrated that ethanol exposure during embryogenesis causes brain abnormalities in several vertebrates, including *X. laevis* (Shi et al., 2014; Yelin et al., 2007; Guizzetti, 2015). Indeed, we found that *X. laevis* specimen exposed to ethanol (during neurulation only) frequently showed mild midline defects in their brains; the olfactory bulbs of the telencephalon were often underdeveloped or fused (Figure 2.1A, Figure 2.1A).

The morphology of the ethanol-exposed tadpole brains at NF stages 45-47 also differed noticeably from control brains in the fact that they frequently displayed midbrain defects and wider hindbrains (Figure 2.1A, Figure 2.1A). Yet, by NF stage 49 the mid and hindbrain morphology of the ethanol tadpoles matched wild-type controls (Figure 2.1A, Figure 2.1A).

Like ethanol tadpoles, the brain morphology of thioridazine tadpoles was pointedly different from controls, at early pre-metamorphic stages. From NF stage 45 to 47, these animals generally displayed wide hindbrains with thin ridges and underdeveloped forebrains and/or midbrains (Figure 2.1A, Figure 2.2A). Strikingly, by NF stage 49 we found that most or all these abnormal morphologies were resolved (Figure 2.1A, Figure 2.2A). As for the ICI 118, 551 tadpole group, at NF stage 45 their brains were fairly normal morphologically, with only slightly underdeveloped telencephalons (Figure 2.1A and Figure 2.2A). Additionally, ICI 118, 551 brains were smaller than those of stage-matched control. Still, by NF stage 49 these animals were indistinguishable from controls based on morphology and size.

Pre-metamorphic tadpoles with malformed brains exhibit increased cell proliferation in brain tissue relative to wild-type tadpoles

Several studies have reported that cell death and cell proliferation are critical for the intense tissue remodeling that occurs during metamorphosis (Schreiber et al., 2001; Ueda, 1996; Brown, 1995). Therefore, we investigated cell proliferation and apoptosis as potential cellular processes through which malformed brain tissue is remodeling and corrected in pre-metamorphic tadpoles.

Through a quantitative analysis of the number of proliferative cells visible from dorsal view images of tadpole brains, we determined that all the experimental groups show a very significant increase in cell proliferation within the brain at NF stage 45 and/or NF stage 47 (Dunn's test; $df = 3$; $p < 0.001$), and no significant difference at stage 49 (Dunn's test; $df = 3$; $p < 0.001$) (Figure 1B). We similarly measured apoptosis in the brains of these experimental animals and found no significant difference, relative to controls at NF stage 45, 47, or 49 (Kruskal-Wallis test; $df = 3$; $p > 0.05$) (Figure 2.2B).

Cerebrospinal fluid (CSF) analysis reveals brain tissue functionality improves along with morphology

Given our observation that the hindbrains of ethanol and thioridazine tadpole groups appeared wider than those of control animals, we decided to investigate whether this was due to the buildup of cerebrospinal fluid (CSF) in the 4^{th} ventricle of the brain. Cerebrospinal fluid is key to the distribution of signaling factors and nutrients throughout the central nervous system and has significant implication for brain development in *X. laevis* (Hagenlocher et al., 2013). Appropriate CSF flow is dependent upon ciliary functionality in the ependymal cells that line the brain ventricles, thus dysfunctional ependymal cells and brain tissue can result in ventricle dilation (hydrocephalus) (Baas et al., 2006; Ibañez-Tallon et al., 2004; Hagenlocher et al., 2013; Banizs et al., 2005; Chiang et al., 2009; Pérez-Fígares et al., 2001).

CSF volume and flow has previously been analyzed in vivo in *X. laevis* embryos and tadpoles via microinjection of fluorescent dyes and microbeads into

the fourth brain ventricle (Mogi et al., 2012; Hagenlocher et al., 2013). Utilizing this approach, we measured cerebrospinal fluid in ethanol, ICI 118,551, and thioridazine tadpole brains (Fig. 2.3). We began by measuring the ratio between the length and width (anterior-posterior [AP] axis to left-right axis [LR] axis) of the 4th ventricle. We found the mean AP:LR ratio of the 4th ventricle was significantly lower in all the experimental groups at NF stage 45, compared to controls (Dunn's test, $df = 3$, $p < 0.05$) (Fig. 3A). This expansion of the ventricular space is consistent with an increase in CSF pressure (Fig. 2.3A,B).

We then analyzed CSF flow by tracking microbead movement within ventricular spaces and quantifying their curvilinear velocities within the forebrain (lateral and 3rd ventricles) and hindbrain (4th ventricle) (Fig.3 B-E). We analyzed CSF flow in the forebrain to determine whether the fused olfactory bulbs seen in ethanol specimen, which remain unresolved, coincided with persistent abnormal CSF flow. Indeed, we found a correlation between the fused forebrain phenotypes in ethanol tadpoles and reduced CSF flow in the forebrain at NF stages 45-50 (Figure 2.3B). Additionally, thioridazine tadpoles with abnormally wide hindbrains had significantly increased CSF flow rate the hindbrain region at NF stage 45-48 (Dunn's test, $df = 3$, $p < 0.01$) (Figure 3F). However, by NF stage 49, CSF flow within the 4th ventricle equalized across the control and experimental groups (Kruskal-Wallis test, $df = 3$, $p < 0.05$) (Figure 2.3F).

Paired box 7 (Pax7) spatial patterning is altered in tadpoles with abnormal brain morphology and normalizes over time

Pax7 is a highly conserved marker for localized cell populations within the central nervous system of tetrapod animals (Moreno et al., 2014; Bandín et al., 2013; Joven et al., 2013). The spatiotemporal patterning of this marker has been thoroughly characterized in embryonic, pre-metamorphic, pro-metamorphic, and adult *X. laevis* tadpole brains (Bandín et al., 2013; Bandín et al., 2014). Thus, we utilized immunohistochemistry to compare Pax7 expression in the brains of our experimental tadpoles and wild-type controls. Allowing for the inspection of tissue differentiation, patterning, and organization in malformed brains as they self-corrected.

Although Pax7 spatial patterning changes dynamically throughout normal brain development, at each developmental stage wild-type controls have a consistent Pax7 expression pattern (Fig. 2.4A). We found that less than 15% of controls deviated from this pattern at any given stage (Fig. 2.4B), whereas 30-45% of ethanol, ICI 118,551, and thioridazine tadpoles displayed atypical Pax7 expression at NF stage 45 (Fig. 2.4A,C-E). The most common case of atypical Pax7 expression observed was reduced (or diffuse) Pax7 pattern along the ridges of the hindbrain ventricle (4^{th} ventricle), as opposed to the sharp punctate expression observed in controls.

Notably, the percentage of tadpoles with abnormal Pax7 spatial patterns in the experimental groups dropped to 10-25% as they progressed to NF stage 49 (Fig. 2.3C-E). While, both the ethanol and ICI 118,551 specimen showed a rather steady improvement in this metric from NF stage 45 to 49, larvae with thioridazine-induced abnormalities showed improvement specifically between NF stage 47 and

49 (Fig. 2.4E). It is also important to note that none of the experimental groups demonstrated ablated Pax 7 patterning, suggesting that cell differentiation within Pax7-positive brain tissue was not drastically altered.

RNA-seq analysis of thioridazine tadpole brain tissue identified differentially expressed hormones and other tissue remodeling factors

Having observed, through several methods, that *X. laevis* larvae are able to resolve malformed brain tissue, we sought to identify and decipher the underlying molecular mechanisms mediating this phenomenon. To that end, we applied a RNAseq-based gene expression analysis on brain tissue isolated from wild-type controls and tadpoles with thioridazine-induced abnormal brain phenotypes. Only the thioridazine treatment was utilized for this approach because it induces very consistent abnormal brain phenotypes that reliably improve over time. Any significant factors identified in thioridazine tadpoles could then be probed in ethanol and ICI 118,551 specimen through RT-qPCR. Differential gene analysis of the RNA-seq run on control and thioridazine brain cDNA libraries revealed 13 differentially expressed genes at stage 45 and 16 at stage 47 (Table 2.1 and 2.2). From the list of differentially expressed genes, we identified factors which correlated with statistically significant upregulation of hormone pathways involving gonadotropin releasing hormone and prolactin hormone in the thioridazine tadpoles, relative to stage matched controls (Table 2.1 and 2.2). We also found significant differential expression of *mmp7* and *col3a1* genes at NF stage 47, both of which are important factors for extracellular matrix remodeling (Table 2.2).

In situ hybridization and RT-qPCR analysis of prolactin.2 confirmed RNAseq results

The RNAseq experiment revealed upregulation of *prolactin.2S* (*prl.2*) in thioridazine-effected brains at NF stage 47. From previous studies in *Xenopus* and other animals we know that prolactin signaling can induce the remodeling of various tissues (Huang et al., 2009; Huang and Brown, 2000a; Jung et al., 2004, Parhar, 2003). Thus, we generated primers specific to the *prolactin.2S* sequence to generate *in situ* RNA probes and further investigate this hormone in experimental tadpoles with brain defects. Analysis of *prl.2* expression through whole-mount *in situ* hybridization revealed relatively normal gene expression patterning, within the hypothalamus and pituitary regions of the brain in all control and experimental groups at pre-metamorphic stages (Fig. 2.5A).

However, through RT-qPCR we found that ethanol and ICI 118,551 tadpoles both showed an approximately 3-fold decrease of *prl.2* at stage 45 and 1.5-fold decrease at stage 47. We also tested the relative expression levels of the *prolactin receptor* gene (*prlr*) and found that at NF stage 47 the ICI 118,551 and ethanol groups showed a 5-fold and 3-fold decrease in *prlr* expression, respectively. As for the thioridazine brain tissue, we noted a 3-fold increase of *prolactin.2* expression in post-thioridazine tadpoles at stage 45 and a 5-fold increase at stage 47, with no change in the expression of *prolactin receptor* at either stage (Figure 2.5). Thus, the RNAseq results were confirmed by RT-qPCR.

Differential mmp1, mmp7, and mmp13 expression occurs in brains undergoing remodeling and repair

Given that our RNAseq experiment discovered increased expression of *prl.2* and *mmp7* in the brain tissue of NF stage 47 thioridazine tadpoles (Table 2.2) and a previous *in vitro* study showing *mmp1 and mmp13* regulation by prolactin signaling (Jung et al., 2004), we examined whether the expression of these three *mmp* genes were also altered in ethanol and ICI 118,551-treated tadpole brain tissue. RT-qPCR revealed 1.5 to 3-fold upregulation of *mmp13* at NF stage 45 in ethanol, ICI 118,551, and thioridazine tadpole brains, as well as 1.5 to 3-fold down regulation of *mmp1* in ICI 118,551 and thioridazine samples (Figure 2.6A). At NF stage 47, the *mmp1* gene also seems to be downregulated in the brain tissue of all three experimental groups (Figure 2.6B).

In order to evaluate the effect that prolactin (*PRL)* signaling may have on the expression levels of *mmp1*, *mmp7*, and *mmp13*, we applied exogenous *X. laevis* Prolactin.2 or pergolide mesylate (an antagonist of *prolactin* gene expression) exposures to wild-type pre-metamorphic tadpoles. Prolactin.2 exposure was expected to bind and activate the prolactin receptor and initiate or upregulate the PRL signaling cascade, based on previous studies which utilized human or ovine prolactin hormone isolates to bind and activate *Xenopus* prolactin receptors (Huang and Brown, 2000b; Campantico et al., 1972). Exposure to pergolide mesylate (PM) was expected to downregulate all *prolactin* gene expression via its agonistic effects on dopamine signaling, ultimately decreasing prolactin hormone prevalence (Fitzgerald and Dinan, 2008; Factor, 1999). Interestingly no significant change in *prl.2.S* gene expression was detected with the PM or PRL.2 exposures (Fig. 2.6C,D). However, we did observe that PM and PRL.2 exposures have opposing

effects on *mmp1, mmp13, and mmp7* expression, with PRL.2 increasing expression and PM decreasing expression (Fig. 2.6C and D). In fact, after only two days of exposures, specimen showed significantly different effects on *mmp1* expression (Fig. 2.6C) (Kruskal-Wallis Test, $df = 2$, $p < 0.05$). After a longer exposure period (7 days), the PM and PRL.2 groups showed significantly opposing effects on all three *mmp* genes (Fig. 6D) (Kruskal-Wallis Test, $df = 2$, $p < 0.05$). Thus, these treatments modulated a factor critical for regulating *mmp1* gene expression, which our evidence suggests is downstream of prolactin signaling.

Discussion

We have characterized brain morphology in pre-metamorphic tadpoles that experienced acute exposures to either ethanol, ICI 118,551, or thioridazine during neurulation. Most craniofacial defect-inducing teratogens affect CNCs; for example, ethanol has been reported to hinder migration and increase apoptosis in the CNCs of frog, fish, murine, and human embryos, all of which develop craniofacial defects (Shi et al., 2014; Guizzetti, 2015; Carvan et al., 2004; Bilotta et al., 2004). Although the mechanisms through which ethanol, thioridazine, and ICI 118,551 induce craniofacial defects are not fully understood, they likely affect apoptosis, proliferation, migration, or differentiation in cranial neural crest cells (CNCs). In fact, ethanol is an antagonist of the retinoic acid signaling pathway, a pathway known to be involved in cell differentiation and patterning of the brain (Yelin et al., 2007). We determined that thioridazine exposure during neurulation

causes obvious brain abnormalities, while exposure to ICI 118,551 has much more subtle effects on brain development.

Through qualitative and quantitative morphological, gene expression, and tissue function analysis, we have found that the ethanol and thioridazine tadpoles have atypical brain morphology and functionality at early pre-metamorphic stages. Intriguingly, if these same analyses are applied to late pre-metamorphic tadpole stages, the experimental tadpole brains match wild-type controls completely or more closely. This is most evident when looking at the morphology, function, and patterning of the 4th ventricle and hindbrain region of thioridazine tadpoles, which drastically improves between NF stage 47 and 49. These results support the existence of an adaptive tissue remodeling and repair mechanism for brain tissue in pre-metamorphic tadpoles (Fig. 2.7). These findings also correlate with, and expand upon, previous reports of the self-correction of craniofacial anomalies in *X. laevis* tadpoles prior to metamorphosis (Vandenburg et al., 2012; Pinet et al. 2019). Ultimately, we find that *X. laevis* specimen exposed to thioridazine during neurulation serve as useful models for the remodeling and repair of malformed craniofacial and brain tissues, due to the consistent effect of acute thioridazine exposure on brain development and the subsequent improvement of malformed brain tissue over time.

This study also highlights cell proliferation and adaptive MMP regulation in brain tissue as potential mechanisms for the remodeling and repair of dysmorphic brain tissue. Our data strongly suggests that cell proliferation is a significant factor in the self-correction of abnormal brain tissue in pre-metamorphic *X. laevis*

tadpoles with brain defects induced via several distinct pharmacological perturbations. During the time period where we see significant changes in brain morphology, for both wild-type and abnormal brains, we also see significant increases in cell proliferation. While, increased proliferation at these developmental stages is associated with growth, it is important to note that tadpoles undergoing self-correction of brain anomalies experience even greater proliferation than their wild-type counterparts. Furthermore, by stage 49/50 at which point brain morphology normalization seems to have ceased, proliferation rates across experimental and control groups are equal. Other remodeling and repair mechanisms that involve proliferation, such as gut remodeling and brain tissue regeneration in *Xenopus laevis*, support the importance of cell proliferation to tissue remodeling in this organism (Ueda, 1996; Heimeier et al., 2010; Gaete et al., 2012).

In addition to characterizing larvae brain tissue before and during self-correction, we applied RNAseq and RT-qPCR to identify some of the genetic factors involved. These factors include *mmp1, mmp13, mmp7,* and *prl.2*. Furthermore, through experimental manipulation of prolactin signaling we have demonstrated a strong link between prolactin signaling and *mmp1* gene regulation, *in vivo*. MMPs are at the heart of tissue remodeling and repair events because they are the major proteinase family responsible for extracellular matrix degradation and turnover in multicellular animals (Visse and Nagase, 2003; Fu et al., 2009; Naitoh et al., 2017; Pinet et al. 2019). Therefore, determining the spatiotemporal protein patterning and function of these MMPs through the design and implementation of antibodies for immunohistochemistries is a natural next step.

Generally, further analysis of the gene cascades responsible for inducing the remodeling and repair of neural tissue in *X. laevis* is required in order to develop detailed models of this phenomenon. However, all that we have uncovered thus far regarding endocrine signaling, *mmp* gene regulation, and cell proliferation profiles in adaptively remodeling brain tissue has significant implications for our understanding of brain development and remodeling in vertebrates. For example, prolactin hormone's effect on neural tissue remodeling and cell behavior in wild-type and atypical specimen certainly deserves further analysis, given our findings and the fact that prolactin has been implicated in the reversal or alleviation of neurodegenerative disease-related symptoms in adult mice and humans (Shingo et al., 2003; Gregg et al., 2007; Costanza and Pedotti, 2016).

Furthermore, previous studies have shown that pre-metamorphic tadpoles can be trained through associative learning and that the ability to learn is hindered in tadpoles with severe brain defects (Blackiston and Levin, 2012; Blackiston and Levin, 2013; Pai et al., 2018). Thus, the increase in cell proliferation observed in self-correcting brain tissue has major consequences, because it could have a positive effect on cognition and learning in these animals. Moving forward, it would be pertinent to determine whether animals with malformed brain tissues have hindered cognitive abilities and whether normalization of the brain tissue restore cognitive abilities. In conclusion, we find that *X. laevis* larvae have a remarkable ability to address and resolve brain abnormalities prior to metamorphosis, via a complex and adaptive molecular mechanism involving endocrine signaling, cell proliferation, and altered *mmp* gene expression.

Experimental Procedures

Embryo culturing and tadpole rearing

All the experiments were conducted in accordance with the guide for Care and Use of Laboratory Animals and were approved by the Institutional Animal Care and Use Committee at Tufts University. Embryo culturing was carried out as previously described by Caine and McLaughlin (Caine and McLaughlin, 2013). Embryos and tadpoles were reared and fed following the methods described in Pinet et al. 2019 (Pinet et al., 2019). Embryos and tadpoles were staged based on Nieuwkoop and Faber (P.D. Nieuwkoop and J. Faber, 1994).

Pharmacological exposures

Embryos were reared at 14˚C until NF stage 13/14, then pharmacological exposures to induce craniofacial defects were conducted on the neurula stage embryos (NF stage 14-26) at 18 ˚C. After the exposures they were kept at 14 ˚C until they reached feeding-tadpole stages. Pharmacological treatments included: 1.5-2% ethanol, 90 µM thioridazine (Tocris), and 25-100 µM ICI 118, 551 (Tocris). Plate densities during exposures were kept at 50 embryos per 10 mL of media.

Cerebrospinal fluid (CSF) flow and volume analysis

CSF flow analysis was based on the procedures previously described by Hagenlocher *et al.* (Hagenlocher et al., 2013). Pre-metamorphic tadpoles were anesthetized with tricaine (MS-222, Sigma) and 10-20 nl injections were made into the fourth brain ventricle using needles made from glass capillaries. The injections solution consisted of a 0.008% FluoSpheres™ (1 µm, yellow-green [505/515], 2%

solids, ThermoFisher), 0.5 µg/µl Dextran, Texas Red ™ (10,000 MW, Neutral, ThermoFisher), and 1x MBSH buffer solution. Fluorescent microbead movement and brain ventricle volume imaging was performed on a Zeiss Axiocam microscope. CSF flow videos were generated by capturing approximately 345 frames over a 5 second window.

Fluorescent microbead velocities were analyzed by isolating 30 consecutive raw frames from the full length CSF flow videos and applying a customized flowcathR package-based R script (Federico Marini, 2015). The temporal color coding, ruler, and polygon outlining features of Fiji were utilized to visualize microbead movement and measure the dimension of the 4th ventricle (Schindelin et al., 2012).

Immunohistochemistry (IHC) and in situ hybridization (ISH)

Tadpoles were euthanized and fixed in 1x MEMFA (0.1 M MOPS, pH 7.4, 2 mM EGTA, 1 mM $MgSO_4$, 3.7% formaldehyde), washed with 1x phosphate buffered saline (PBS), dehydrated in methanol, bleached overnight at room temperature with a 9% hydrogen peroxide solution under a constant light source, transitioned to 100% methanol, and stored at -20˚C until used for IHC or ISH. Whole-mount IHC and ISH were performed as described by Caine and McLaughlin (Caine and McLaughlin, 2013), except IHC on brain tissue often required that we dissect out the brain prior to incubation with IHC antibodies, resulting in a whole-brain rather than whole-mount approach. The IHC primary antibodies utilized for this study were, 12/101 (skeletal muscle marker; Developmental Studies Hybridoma Bank [DSHB]), anti-PAX7 (neural marker; DSHB), anti-

phosphorylated histone 3 (pH3, mitotic cell marker; Thermo Fisher Scientific), and anti-active Caspase 3 (apoptotic cell marker; BD Biosciences Pharminogen). The IHC secondary antibodies used were either goat anti-mouse of goat anti-rabbit conjugated to alkaline phosphatase (AP; 1:1,500 dilution, Sigma), Alexa Fluor 488 (AF488; 1:300 dilution, Abcam), or Alexa Fluor 555 (AF555; 1:300 dilution, Abcam). The ISH transcripts detected were *PRL.1.L and PRL.2.S*, see supplementary table 1 for RNA probe sequences.

For sectioning of brain tissue post IHC, isolated brains were embedded in 4% agarose solution, then sectioned on a Leica vibratome. The 75 µM sections were then cleared in a 50% glycerol: 50% PBS solution and mounted on slides for imaging on a Nikon SMZ1500 dissections microscope with a Spot Insight Color digital camera and Spot Image Solutions^{TM} software.

Real time quantitative PCR (RT-qPCR) and RNA-Seq

RNA libraries were generated from brain tissue and RNAseq cDNA libraries were generated following methods described in Pinet *et. al.* 2019 (Pinet et. al. 2019). Isolated brain tissue RNAseq cDNA libraries were pooled and run on Illumina Hi-Seq 2500 at the Tufts University Core Facility to generate 100-bp single end reads. The sequencing reads were then trimmed to remove adapter sequences and filtered to remove any low-quality reads with Trimmomatic, then mapped to the *Xenopus laevis* genome v9.1 with HISAT2. Transcript count tables were generated with HTSeq-count and differential gene analysis was carried out using the DESeq2 package in R (Love et al., 2014).

Statistics

For sufficient statistical power, a minimum total samples size (total n) of 14 tadpoles per control and experimental group was applied; total n is the sum of samples sizes (n) across multiple biological replicates (N). Quantitative data across multiple control and experimental groups were analyzed with Kruskal-Wallis non-parametric tests (KW test), if the KW test were significant, a post-hoc Dunn's test was performed. Bonferroni p-value adjustments were also utilized to adjust for multiple testing bias.

Acknowledgements

We appreciate the helpful discussions with members of the McLaughlin and Levin labs, as well as many others in the developmental biology field. We acknowledge support from an Allen Discovery Center award from the Paul G. Allen Frontiers Group (No. 12171).

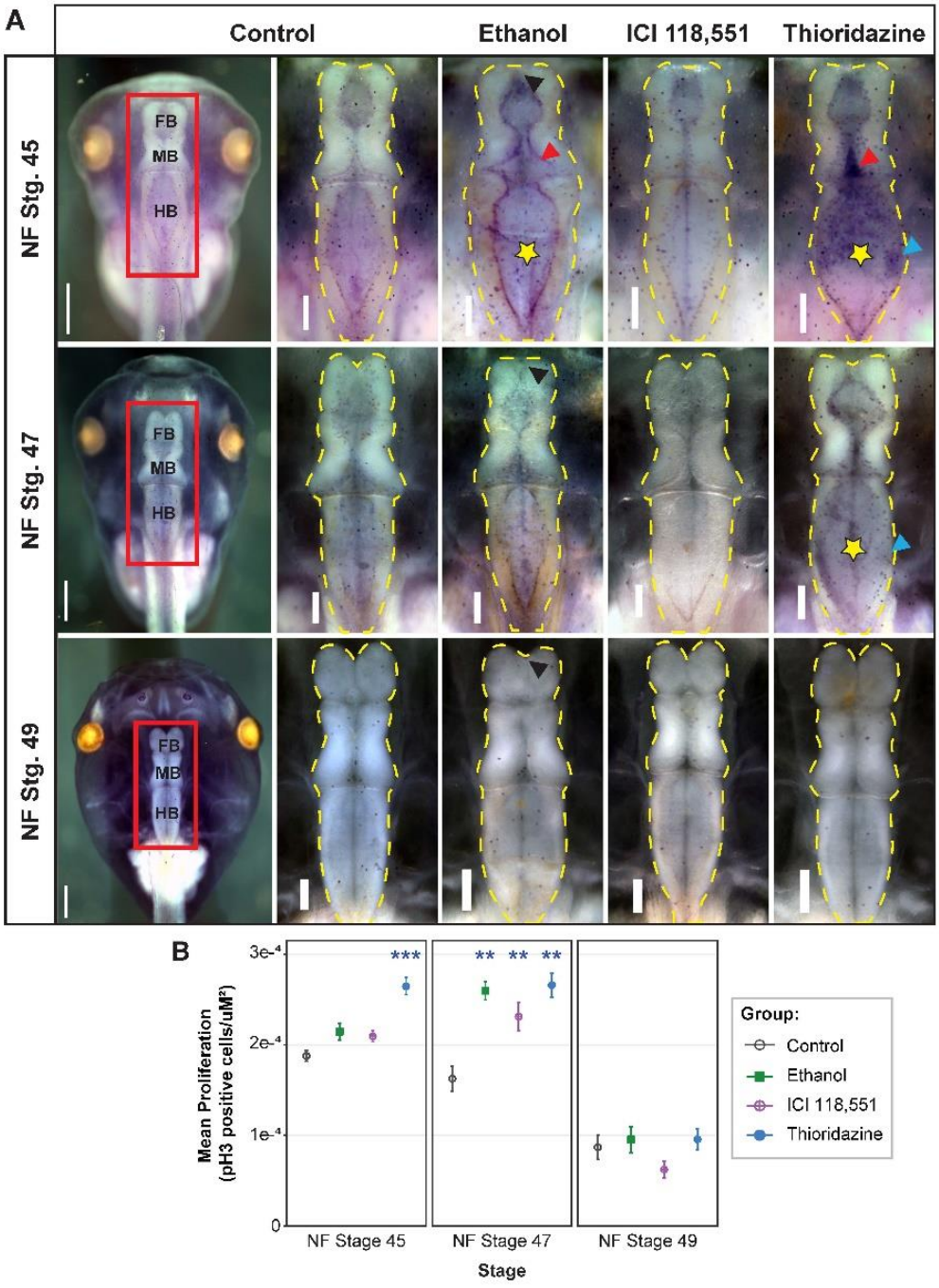

Figure 2.1. Thioridazine and ethanol tadpoles show normalized brain morphology between NF stage 45 and 49, after experiencing increased cell proliferation across brain tissue.

Figure 2.1. Thioridazine and ethanol tadpoles show normalized brain morphology between NF stage 45 and 49, after experiencing increased cell proliferation across brain tissue. A) Immunohistochemistry for phosphorylated-histone 3 (pH3); a cell proliferation marker. Representative NF stage 45, 47, and 49 control, ethanol, IC 118,551, and thioridazine tadpole brains, respectively. Blue, red, and black arrowheads point to fused olfactory bulbs, malformed midbrain, and thin hindbrain ridges, respectively. Yellow stars signify abnormally wide hindbrain ventricle. Scale bar for whole head images = 500 µM. Scale bar for brain images = 200 µM. FB = Forebrain; MB = Midbrain; HB = hindbrain. B) Quantified mean proliferation ± standard error (pH3 positive cells/μM^2) in control, ethanol, ICI 118,551, and thioridazine brains, measured from dorsal view images at NF stage 45, 47, and 49, respectively. Kruskal-Wallis tests were followed by Dunn's post-hoc test when appropriate; ***$p < 0.001$, **$p < 0.01$ for Dunn's post-hoc test. N = 3, n = 8-29, for a total n of 41-65 for each group/stage.

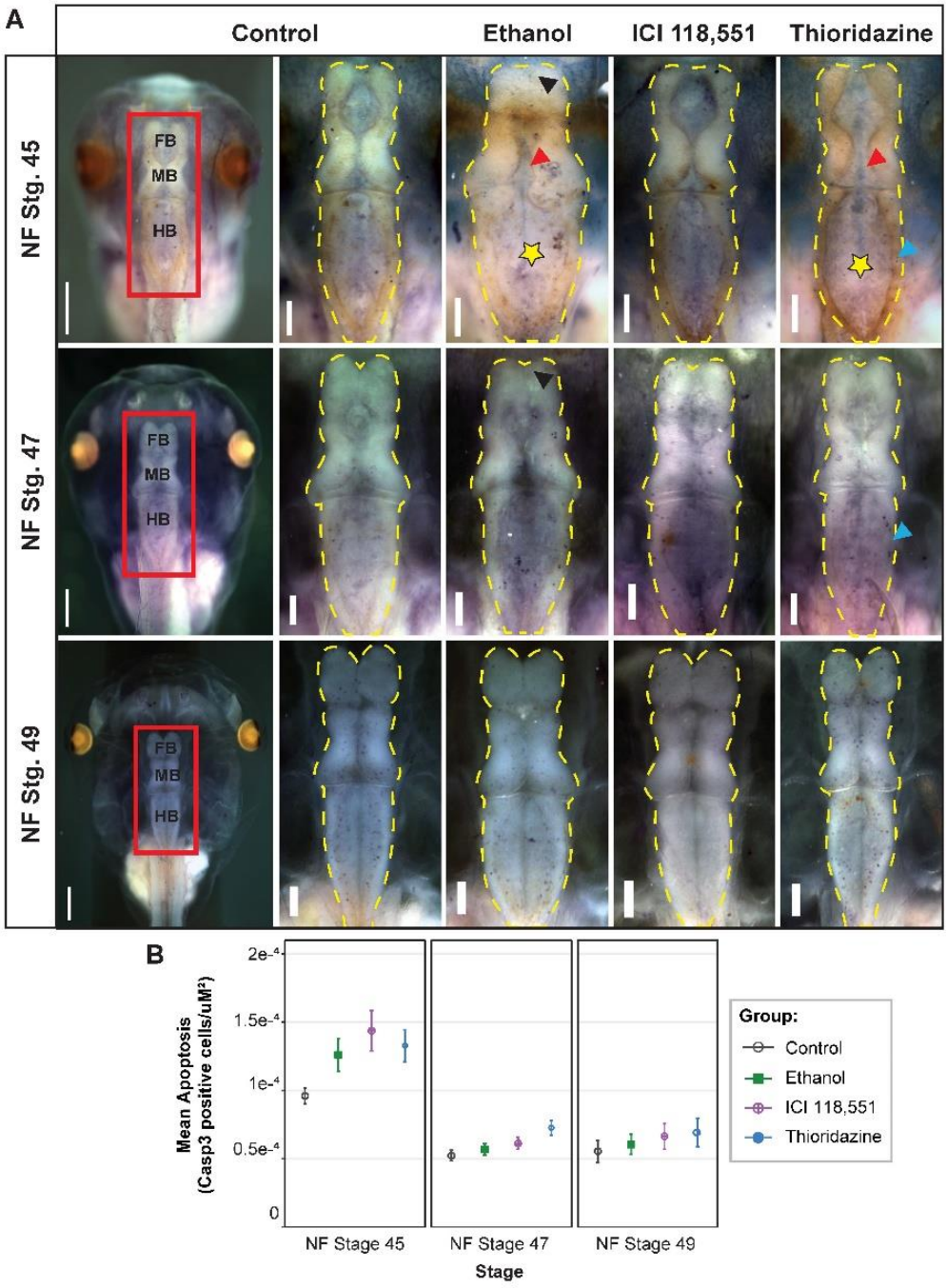

Figure 2.2. Ethanol, ICI 118, 551, and thioridazine tadpoles do not show significantly increased apoptosis across brain tissue, relative to controls between NF stage 45 and 49.

Figure 2.2. Ethanol, ICI 118, 551, and thioridazine tadpoles do not show significantly increased apoptosis across brain tissue, relative to controls between NF stage 45 and 49. A) Immunohistochemistry for alpha-caspase 3 (Casp3); a cell apoptosis marker. Representative NF stage 45, 47, and 49 control, ethanol, ICI 118,551, and thioridazine tadpole brains, respectively. Blue, red, and black arrowheads point to fused olfactory bulbs, malformed midbrain, and thin hindbrain ridges, respectively. Yellow stars signify abnormally wide hindbrain ventricle. Scale bar for whole head images = 500 µM. Scale bar for brain images = 200 µM. FB = Forebrain; MB = Midbrain; HB = hindbrain. B) Quantified mean apoptosis ± standard error (Casp3 positive cells/μM^2) in control, ethanol, ICI 118,551, and thioridazine brains, measured from dorsal view images at NF stage 45, 47, and 49, respectively. Kruskal-Wallis tests for all stage revealed no significant difference between groups ($p > 0.05$). N = 3, n = 8-17, for a total n of 36-46 for each group/stage.

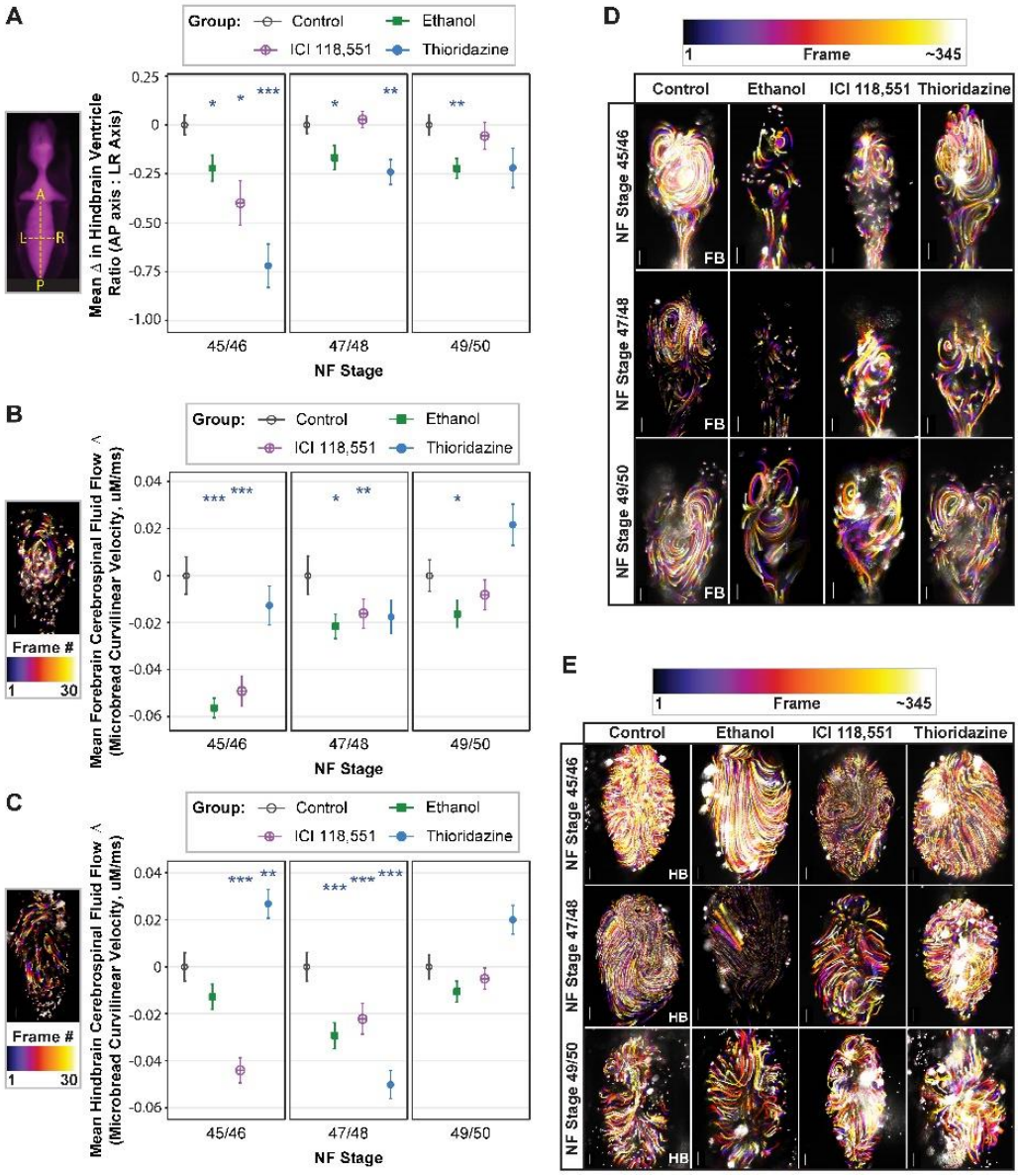

Figure 2.3. Ventricular expansion and altered cerebrospinal fluid (CSF) flow correspond with abnormal brain phenotypes.

Figure 2.3. Ventricular expansion and altered cerebrospinal fluid (CSF) flow correspond with abnormal brain phenotypes. A) Analysis of difference in the fourth ventricle length to width ratio (anterior-posterior axis [AP] to left-right axis [LR] ratio) between controls and experimental tadpoles. B) Quantified difference in forebrain CSF flow (microbead curvilinear velocity, μM/ms) in ethanol, ICI 118,551, and thioridazine brains, relative to controls. Curvilinear velocity was measured from dorsal view videos at NF stage 45-50. C) Same analysis as B, except on the hindbrain ventricle. D,E) Pseudo-colored trajectories generated from time-lapse images taken over 5 seconds of fluorescent microbeads within the forebrain and hindbrain ventricles, respectively. Darker trajectories correspond with shorter distance traveled across ~345 frames (~5 seconds), while lighter trajectories correspond with larger distances traveled across ~345 frames. For ventricle volume experiments, N = 3, n =14-22 , for a total n of 43-65 for each group/stage. For CSF velocity experiments, N = 3-5, n = 4-7, for a total n of 14-33 for each group/stage. Kruskal-Wallis tests were followed by Dunn's post-hoc test when appropriate; ***$p < 0.001$, **$p < 0.01$, *$p < 0.05$ for Dunn's post-hoc test. Scale bars in forebrain and hindbrain microbead trajectory images equal 100 μM.

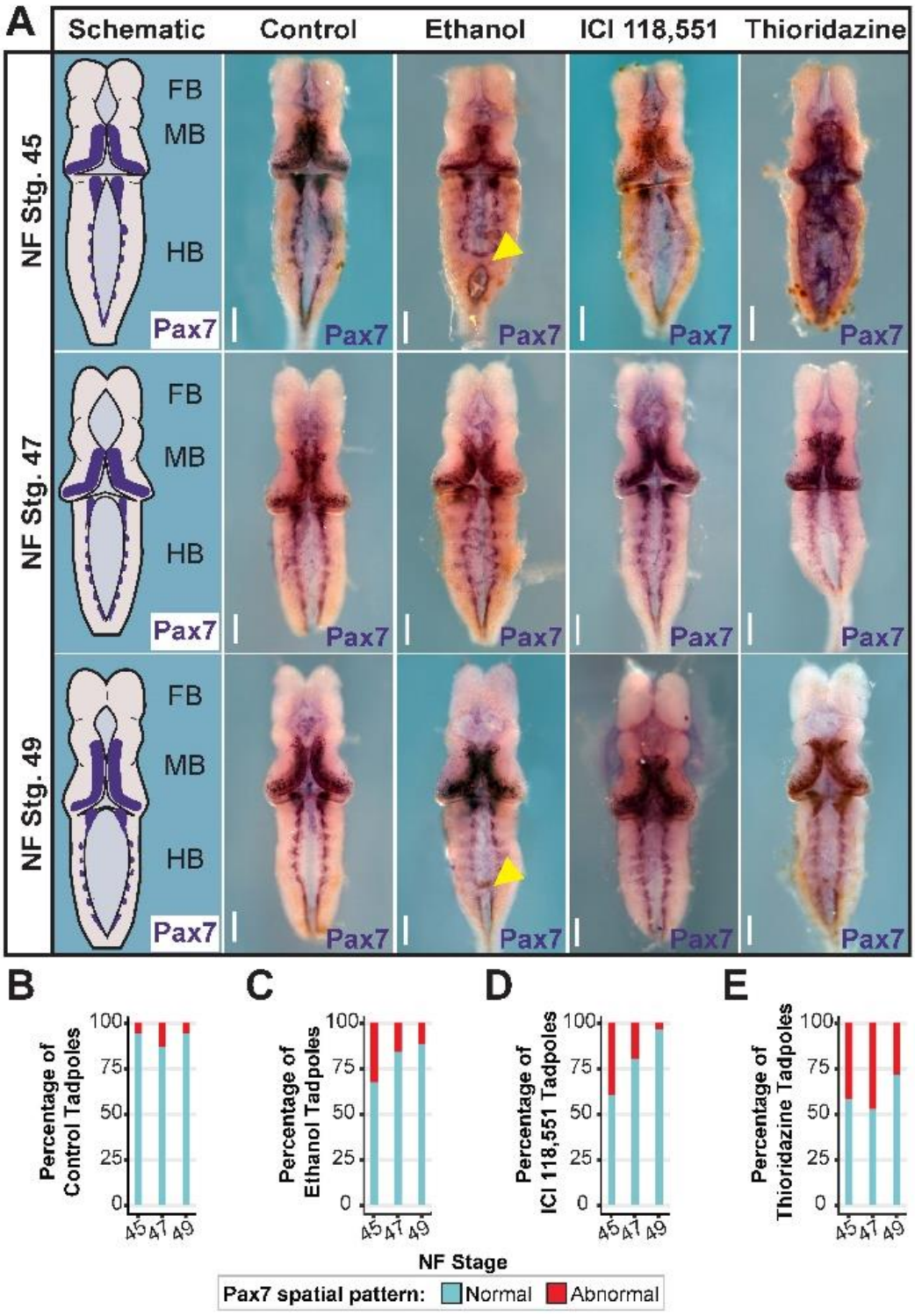

Figure 2.4. Paired box 7 (Pax7) immunohistochemistry reveals abnormal neural tissue patterning in ethanol and thioridazine exposed tadpoles at NF stage 45, which is largely resolved by NF stage 49.

Figure 2.4. Paired box 7 (Pax7) immunohistochemistry reveals abnormal neural tissue patterning in ethanol and thioridazine exposed tadpoles at NF stage 45, which is largely resolved by NF stage 49. A) Control, ethanol, ICI 118,551, and thioridazine whole-brain-mount immunohistochemistry for Pax7 at NF stage 45, 47, and 49. Pax7 is a marker for neural cells within the midbrain and hindbrain regions. Images are representative of phenotypes seen over three trials. Yellow arrow heads point to ectopic brain tissue and Pax7 expression. N=3, n= 8, for a total n of 24 for each group/stage.

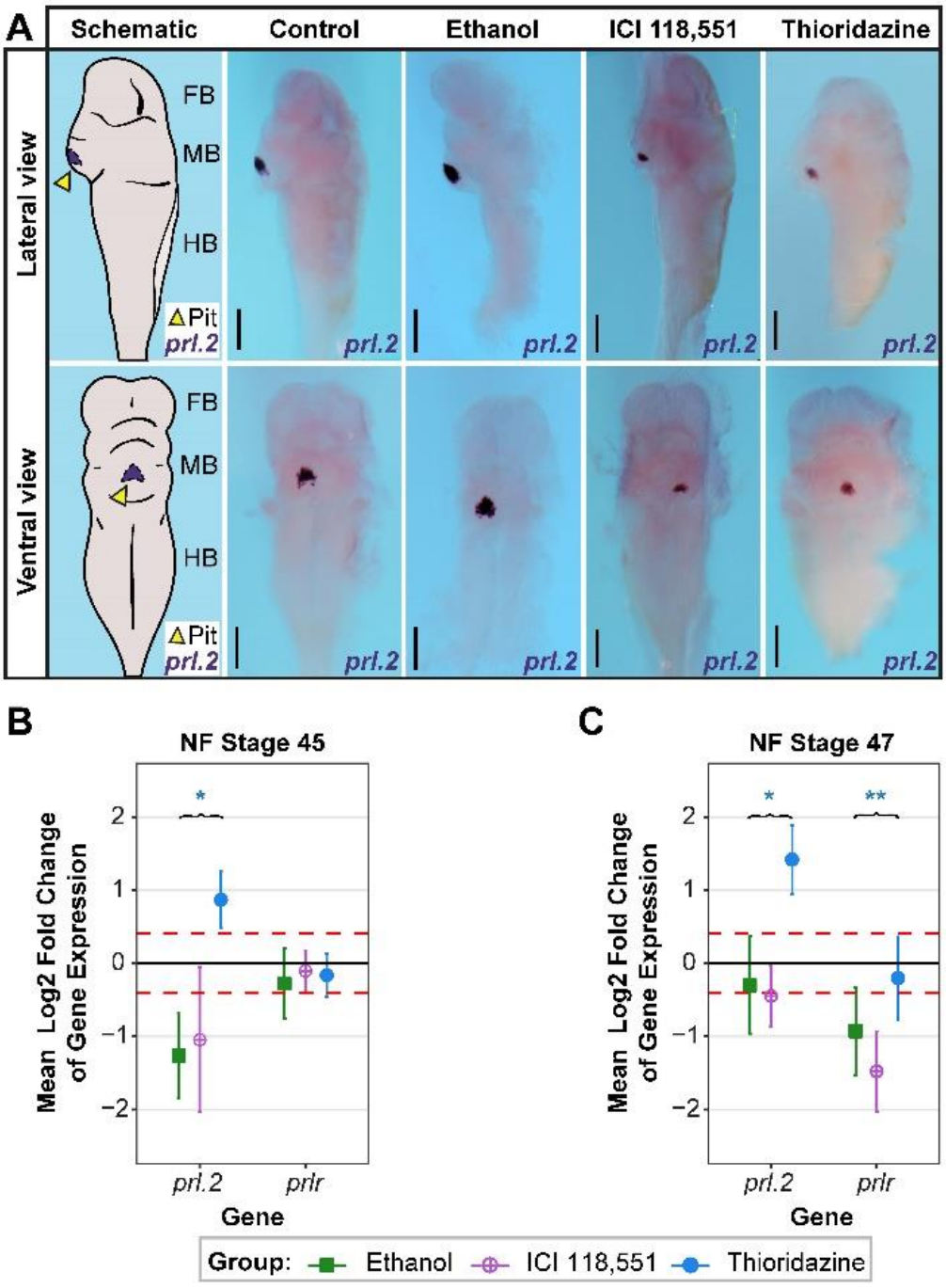

Figure 2.5. Whole-mount *in situ* hybridization and RT-qPCR confirms *Prl.2* is expressed in the hypothalamic and pituitary regions of pre-metamorphic wild-type, ethanol, ICI 118,551, and thioridazine tadpole brains.

Figure 2.5. Whole-mount *in situ* hybridization and RT-qPCR confirms *Prl.2* is expressed in the hypothalamic and pituitary regions of pre-metamorphic wild-type, ethanol, ICI 118,551, and thioridazine tadpole brains. A) Lateral and ventral views of Isolated brains from *Prolactin.2* (*Prl.2*) whole-mount *in situ* hybridization on control, ethanol, ICI 118,551 and thioridazine tadpoles. B & C) RT-qPCR for *Prl.2* and *Prlr* gene expression in control (y = 0), ethanol, ICI 118,551, and thioridazine brain tissue at NF stage 45 and 47, respectively. Gene quantity was normalized by eukaryotic elongation factor 1 alpha (*eef1a*a) expression values, then by matching control values. Thus, control mean log2 fold change values are set to zero. *$p < 0.05$, **$p < 0.01$ for Kruskal-Wallis test. N= 3, n=10 for each group/stage.

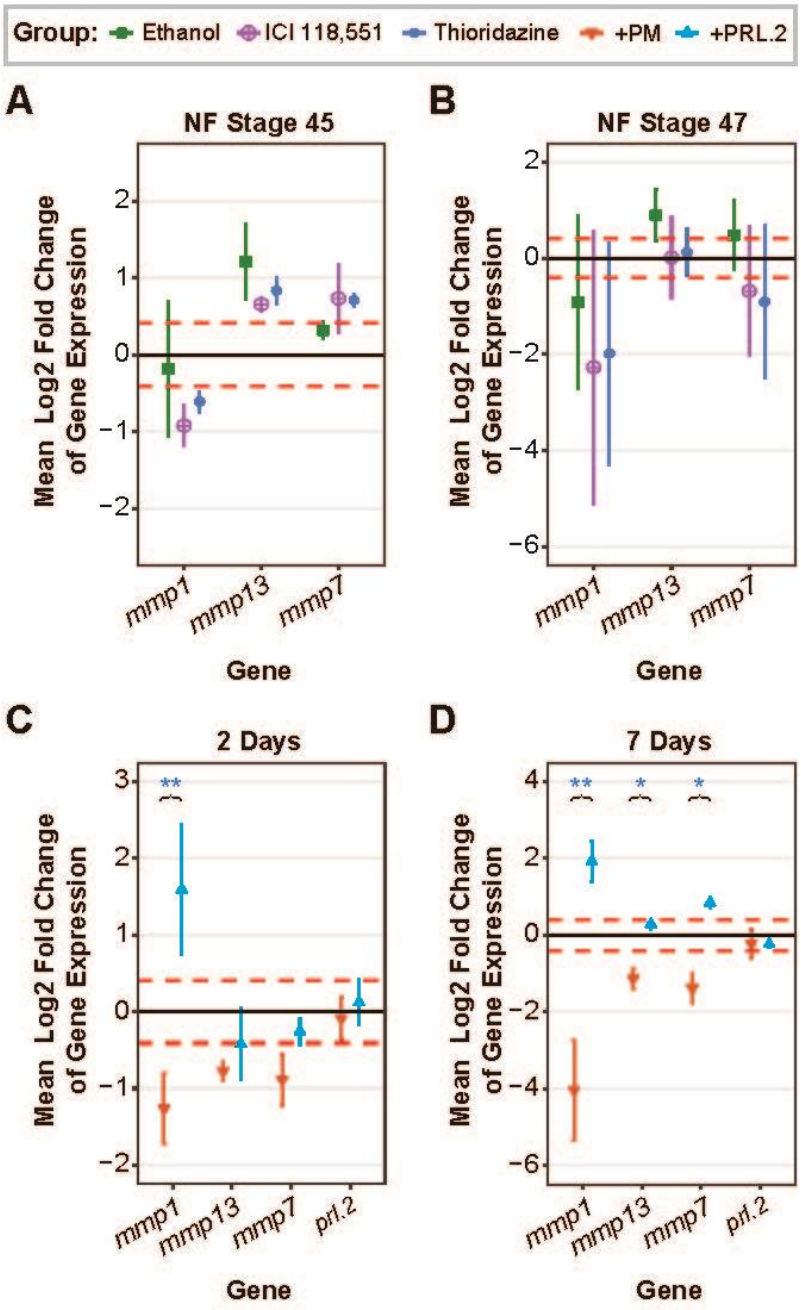

Figure 2.6. RT-qPCR reveals differential *mmp1*, *mmp7*, and *mmp13* regulation in brain tissue undergoing adaptive tissue remodeling and repair, which cannot be fully recapitulated in wild-type control brains through modulation of Prolactin signaling.

Figure 2.6. RT-qPCR reveals differential *mmp1*, *mmp7,* and *mmp13* regulation in brain tissue undergoing adaptive tissue remodeling and repair, which cannot be fully recapitulated in wild-type control brains through modulation of Prolactin signaling. A & B) RT-qPCR for *mmp1*, *mmp13*, and *mmp7* in control (y = 0), ethanol, ICI 118,551 , and thioridazine brain tissue samples at NF stage 45 and 47, respectively. C & D) RT-qPCR for *mmp1*, *mmp13*, *mmp7, and prl.2* in wild-type (control, y = 0), wild-type + pergolide mesylate (+PM), and wildtype + Prolactin.2 (+PRL.2) tadpoles after 2 and 7 days of continuous exposures, respectively. Gene quantity was normalized by eukaryotic elongation factor 1 alpha (*eef1a*a) expression values, then by matching control values. Thus, control mean log2 fold change values are set to zero. *$p < 0.05$, **$p < 0.01$ for Kruskal-Wallis test. N= 2-3, n=10 for each group/stage.

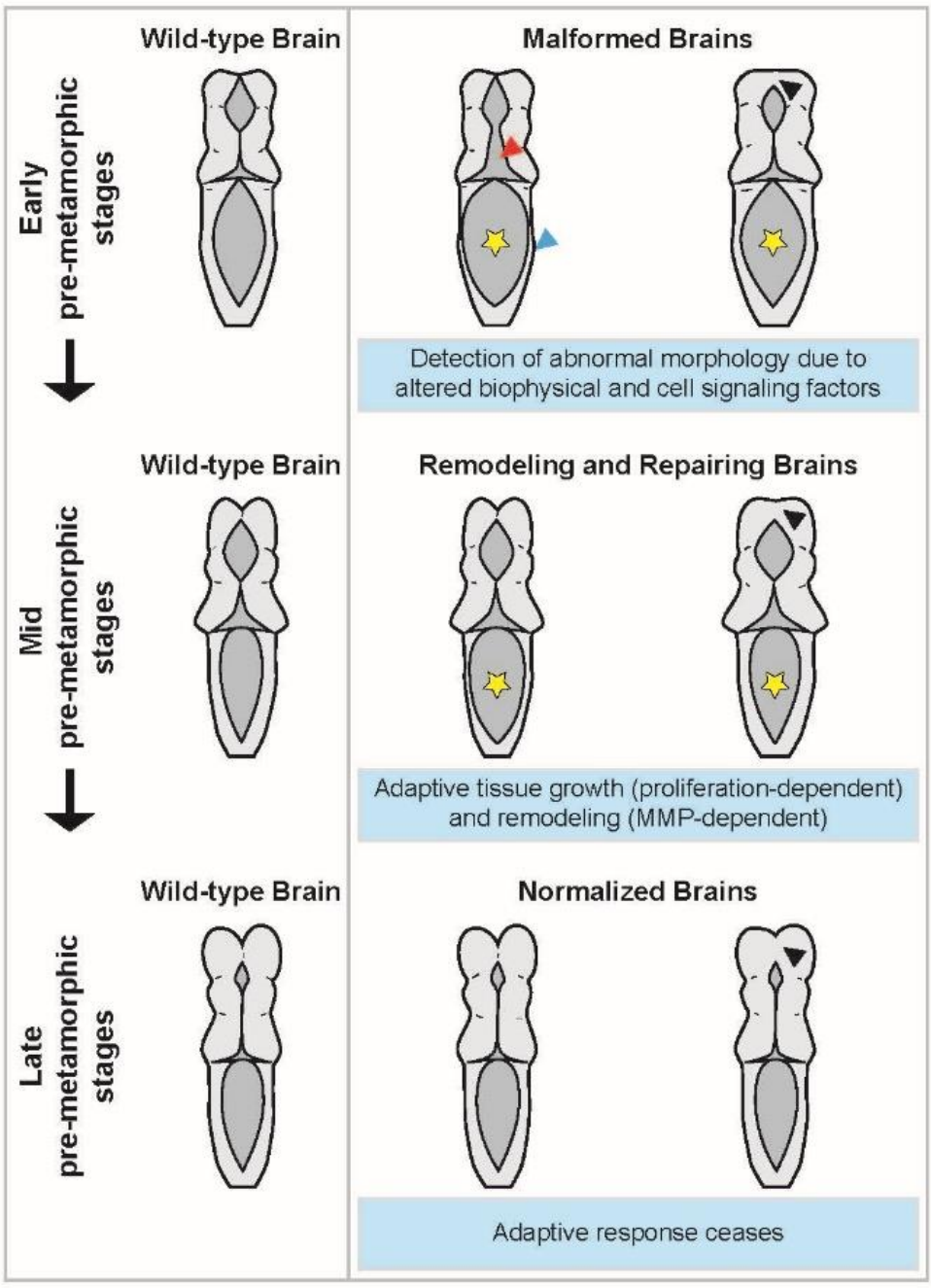

Figure 2.7. Model for the adaptive tissue remodeling and repair response observed in pre-metamorphic *X. laevis* tadpoles with abnormal brain morphology.

Figure 2.7. Model for the adaptive tissue remodeling and repair response observed in pre-metamorphic *X. laevis* tadpoles with abnormal brain morphology. Adaptive brain tissue remodeling and repair primarily occurs between NF stage 47 and 49, during which malformed brains experience an increase in cell proliferation and *mmp* gene expression. Afterwards, brain morphology is normalized and may not be differentiable from stage-matched wild-type brains. Blue, red, and black arrowheads point to fused olfactory bulbs, malformed midbrain, and thin hindbrain ridges, respectively. Yellow stars signify abnormally wide hindbrain ventricle.

Table 2.1. Thirteen differentially expressed genes between control and post-thioridazine brain tissue samples at NF stage 45 found through RNAseq. N = 3, n = 10 brains per group/stage.

Gene Symbol	GenBank Gene Accession	log2 Fold Change (Mean ± SE)	Adjusted P Value
c1qtnf9b.L	XR_001934332	6.51 ± 1.015	$4.280E^{-06}$
MGC64358	NM_001086304	4.84 ± 1.003	$6.831E^{-03}$
slc34a3.L	XM_018229375	4.50 ± 0.924	$6.721E^{-03}$
adh7.S	NM_001093434	4.46 ± 0.847	$1.214E^{-03}$
slc23a1.L	XM_018251343	4.23 ± 0.950	$2.311E^{-02}$
LOC108715679	XM_018261058	3.61 ± 0.815	$2.329E^{-02}$
cltrn.L	XM_018244790	3.39 ± 0.738	$1.792E^{-02}$
LOC495407	NM_001095065	3.33 ± 0.635	$1.214E^{-03}$
rgn.S	XM_018249822	1.73 ± 0.379	$1.955E^{-02}$
LOC108718490	XM_018266824	1.61 ± 0.359	$2.311E^{-02}$
LOC108719682	XM_018268871	1.60 ± 0.358	$2.311E^{-02}$
slc24a5.L	XM_018253090	1.20 ± 0.292	$9.806E^{-02}$
gnrh2.L	XM_018227027	1.11 ± 0.210	$1.214E^{-03}$

Table 2.2. Sixteen differentially expressed genes between control and post-thioridazine brain tissue samples at NF stage 47 found through RNAseq. N = 3, n = 10 brains per group/stage.

Gene Symbol	GenBank Gene Accession	log2 Fold Change (Mean ± SE)	Adjusted P Value
LOC100495517.S	NM_001089905	5.69 ± 1.129	0.003
LOC108715679	XM_018261058	3.21 ± 0.750	0.040
LOC108698356	XM_018229778	2.90 ± 0.697	0.062
rgn.L	NM_001085655	2.62 ± 0.651	0.100
LOC108713473	XM_018257041	1.95 ± 0.432	0.018
LOC108709516	XM_018249437	1.88 ± 0.423	0.022
gpnmb.L	NM_001095618	1.32 ± 0.284	0.012
prl.2.S	XM_018227169	1.25 ± 0.209	$6.470E^{-05}$
MGC53823	NM_001086195	0.93 ± 0.212	0.029
epx.L	NM_001088379	0.90 ± 0.181	0.003
elf3.S	XM_018249348	0.89 ± 0.165	0.001
mmp7.L	NM_001086213	0.81 ± 0.179	0.018
mpo.L	XM_018244848	0.80 ± 0.172	0.012
col3a1.S	NM_001090075	0.71 ± 0.126	0.000
gpr151.L	XM_018252147	-0.74 ± 0.178	0.062
krt61.L	XM_018245249	-1.36 ± 0.292	0.012

Table S2.1. *PRL2* and *PRL1* sense and antisense RNA *in situ* probe sequences.

Probe	Sequence
Sense *PRL.2.S*	ccactttgtacaagaaagctgggtacgcgtaagcttgggcccctcgaggg atactctagagcGGCCGCATGGCCAGCTCAAGAAGAGGTATCATGCTCCT TGCACTGTTGATGTCTGATGTGTTTGTGATGAGAAAGATGGTATCCTCTA TGCCAATATGTACTCCTGGAAGCTTCCAGTGTCAGGTTCTGCTTAGTGAC CTCTTCGACAGAGCTATAAAGTTATCACACTATATCCATTCCCTGTCCAC AGAGATGTATGAGGACCTGGATCAGAGGTTTTCCCAAGGCCGTCAGATTT TAGGGAAAGCCATGATCAGCTGTCACACCTCCTCCCTAAGTACCCCAGAG GACAAGGACCAGGCTTTGCAGACACACCATGACGACCTGATTAACCTTGT GCAGAAGTTACTGCGCTCATGGAACCAGCCCTTACAACATTTGGCACTGG AGGCTCCAGACAACATGGCGAGCAAAATGAAAGAAGTTGAGGAGCATGCA AAGATCCTGCAGGGAGGGATTGATAGGATTGCTGGAAGGATGCAAAGCAA TCTGGGAGATGAATTCTACCCTCAATGGCTCACCCCGGGGGATTCCAGGA TGCCAAATGGAGATTCTGAGAGTTATGCCCTCTATCACTTACTGCACTGT TTCCGGAGGGATTCCAACAAGATAGACAACTACCTGAAGATCCTCCGCTG CCGCATGGTGCACGCCAGCAACTGCAGGg
A.S. *Prl.2.S*	caagtttgtacaaaaaagcaggctggtaccCCTGCAGTTGCTGGCGTGCA CCATGCGGCAGCGGAGGATCTTCAGGTAGTTGTCTATCTTGTTGGAATCC CTCCGGAAACAGTGCAGTAAGTGATAGAGGGCATAACTCTCAGAATCTCC ATTTGGCATCCTGGAATCCCCCGGGGTGAGCCATTGAGGGTAGAATTCAT CTCCCAGATTGCTTTGCATCCTTCCAGCAATCCTATCAATCCCTCCCTGC AGGATCTTTGCATGCTCCTCAACTTCTTTCATTTTGCTCGCCATGTTGTC TGGAGCCTCCAGTGCCAAATGTTGTAAGGGCTGGTTCCATGAGCGCAGTA ACTTCTGCACAAGGTTAATCAGGTCGTCATGGTGTGTCTGCAAAGCCTGG TCCTTGTCCTCTGGGGTACTTAGGGAGGAGGTGTGACAGCTGATCATGGC TTTCCCTAAAATCTGACGGCCTTGGGAAAACCTCTGATCCAGGTCCTCAT ACATCTCTGTGGACAGGGAATGGATATAGTGTGATAACTTTATAGCTCTG TCGAAGAGGTCACTAAGCAGAACCTGACACTGGAAGCTTCCAGGAGTACA TATTGGCATAGAGGATACCATCTTTCTCATCACAAACACATCAGACATCA ACAGTGCAAGGAGCATGATACCTCTTCTTGAGCTGGCCATGCGGCC

CHAPTER THREE

Conclusions and future directions

Summary of thesis work

In this thesis, I have focused on the characterization of brain tissue before, during and after the self-correction process that is seen in pre-metamorphic *Xenopus laevis* tadpoles. I sought out to answer three main questions: (1) Does abnormal brain structure cause abnormal cerebrospinal fluid flow and can this be corrected? (2) Are abnormal protein expression patterns corrected over time?, and (3) Is tissue remodeling involved? In the McLaughlin lab, a principle goal is to elucidate the mechanism by which pre-metamorphic tadpoles with craniofacial abnormalities self-correct over time, in the hope that this information could be used to create better treatments for human beings born with facial deformities. We examined cerebrospinal fluid flow, Pax7 protein expression patterns, and *mmp* gene regulation to better understand the process that leads to the normalization of craniofacial deformities in *Xenopus laevis* tadpoles.

The results of this study showed that both cerebrospinal fluid and protein expression patterns can be used as markers for the self-correction of craniofacial abnormalities in *Xenopus laevis* pre-metamorphic tadpoles. The CSF data showed abnormal brain morphologies do correspond with abnormal CSF flow, and this normalizes over time. The Pax7 data showed that region-specific markers of tissue differentiation normalize over time in pre-metamorphic stages.

Preliminary studies done in the McLaughlin lab had shown that brain morphologies in all three of the treatment groups appeared to improve prior to metamorphosis. It was observed during these experiments that many of the malformed brains exhibited expanded hindbrains, specifically in the 4th ventricle, with thinner edges along the hindbrain. It was hypothesized that there was some

kind of blockage within the malformed brains that was not allowing cerebrospinal fluid to flow freely, causing a buildup of this fluid in the hindbrain. Therefore, we wanted to examine the cerebrospinal fluid flow in control, ICI 118,551 HCl, thioridazine HCl, and ethanol tadpole brains to show whether there were measurable differences in the treated brains, and whether they could be corrected. An alteration in cerebrospinal fluid could have large impacts on the health of the organism overall, because cerebrospinal fluid is involved in nutrient and waste control and has a role as a "broadcasting system" to send signals to various parts of the brain (Veening et al., 2010).

While altered cerebrospinal fluid flow was found in the forebrains of tadpoles with misshaped fore and hindbrains, the overall volume of cerebrospinal fluid in the treated brains was not found to be significantly different form that of the control brains. However, further analysis of the brain size and shape revealed that the treated brains are smaller overall than the control brains. Since they still contain the same volume of cerebrospinal fluid within a smaller space, the pressure from the fluid is greater in the treated brains, likely causing the distortions seen in the hindbrains.

After examining the physical brain tissue phenotype and function, I wanted to explore whether cell level differentiation was altered in the experimental groups and if brain tissue pattering improved over time, as the cerebrospinal fluid flow did. I did so by performing the immunohistochemistry procedure on control, ICI 118,551 HCl, thioridazine HCl, and ethanol tadpole brains using Pax7 antibodies to determine how similar brain tissue in the

treatment groups is to that of control groups. Pax proteins have been found to be essential during development, and are involved in neuronal proliferation, brain regionalization, cell differentiation, and neuronal survival (Bandín, et al. 2013). Pax7 is involved in early brain regionalization and maintenance of identity, and it is expressed in both humans and *Xenopus laevis* (Bandín et al., 2013). In fact, there is an extremely conserved distribution pattern of Pax7 cells between amphibians and other vertebrates (Bandín et al., 2013). The Pax7 protein is found primarily in the midbrain and hindbrain of pre-metamorphic *Xenopus laevis* brains (Bandín et al., 2013). Thus, we used Pax7 as a marker for proper differentiation of the midbrain and hindbrain regions.

These results indicated that Pax7 protein expression in certain tadpoles with craniofacial defects is different from the Pax7 expression seen in control brains at stage 45. However, the treatment groups with brains that show miss-patterned Pax7 expression generally become increasingly similar to controls over time (matching controls by stage 49). This is particularly true for the brains of tadpoles from the ICI 118,551 and ethanol groups. Thus, our study revealed that abnormal brain morphology in pre-metamorphic *Xenopus laevis* tadpoles can improve over time, along with the improvement of overall head morphology. While the improvement of abnormal head morphology in these animals was previously observed by Vandenberg et al., brain morphology was not examined (Vandenberg et al., 2012).

We then wanted to investigate the genetic factors involved in the self-correction of malformed brain tissue. An RNAseq experiment by the McLaughlin

lab on thioridazine-HCl exposed brains revealed an upregulation of *prolactin.2S* and *mmp7* so we decided to examine the expression of these genes, as well as *mmp1* and *mmp13*, during the remodeling and repair process occurring in these tadpoles. From this work we confirmed that *prolactin.2.S* expression is upregulated in thioridazine tadpole brains and that *mmp* genes are differentially regulated in self-correcting tadpole head and brain tissue.

We followed up on these findings by investigating Prolactin.2.S hormone's influence on *mmp* gene expression. In the 2000s, it was discovered that increased prolactin signaling modulates *mmp1* and *mmp13* expression in *ex vivo X. laevis* cell culture experiments (Jung et al., 2004). However, in *Xenopus laevis*, there are four different *prolactin* gene variants within the *Xenopus laevis* genome (Session et al., 2016). The McLaughlin lab recently generated Prolactin.2.S (PRL.2.S) extracts, so we could investigate how exogenous Prolactin.2.S exposure altered *mmp* expression *in vivo*. As a negative control, we used pergolide mesylate (PM) exposure to downregulate all prolactin gene expression and signaling in tadpoles. Through RT-qPCR, it was found that PRL.2 upregulated all three *mmp* genes, having a particularly strong influence on *mmp1*, while PM downregulated all three *mmp* genes. The upregulation of *mmp* genes, especially *mmp1* in brains that were exposed to PRL.2 suggests that thioridazine HCl-exposed brains undergoing remodeling and repair have significantly different levels of MMPs than normal, indicating that they could be involved in the self-correction process that we observe in *Xenopus laevis* tadpoles.

A possible explanation for the upregulation of *mmp* gene expression

could be that this process is an inflammatory response of *Xenopus laevis* tadpoles. MMPs have been shown to play a pivotal role in retinal regeneration and suggest that inflammatory cytokines trigger MMP upregulation (Naitoh et al., 2017). It is possible that the increased pressure within the brain due to hydrocephalus may trigger an inflammatory response that causes the upregulation of *mmp* genes, indicating that there is a self-correction procedure set in place in these organisms that can be initiated in the event of craniofacial malformations.

Overall, this study has expanded our knowledge of the ability of the tadpole brain to normalize over time when malformations are induced through chemical treatments. We now understand that the abnormal brain morphologies we observed correspond with abnormal brain tissue patterning as well as hydrocephaly. We have shown that *Xenopus laevis* tadpoles self-correct both of these types of abnormalities using a specific response mechanism prior to and separate from metamorphosis. The qPCR data suggests that this mechanism involves *prl.2* and the upregulation of *mmp* genes, especially *mmp1*. In the end, this study has brought us closer to elucidating the mechanism by which *Xenopus laevis* pre-metamorphic tadpoles are able to fix head and brain malformations on their own. The discovery of this mechanism would lead to the development of more effective, less invasive treatment methods for human beings with craniofacial malformations.

Significance and broader implications

This thesis presented novel information on the ability of pre-metamorphic *Xenopus laevis* tadpoles to remodel malformed brain tissue. Tadpoles with brain malformations can normalize tissue morphology, cerebrospinal fluid flow, and tissue patterning over time. Because of this study, we have concrete evidence that this self-correction of brain irregularities does occur. In addition, we have learned that prolactin hormone and *mmp* regulation play a role in the mechanism that controls the self-correction of craniofacial malformations. The significance of these results is that we now understand key molecular components of the mechanism that allows for this remodeling of malformed tissue and causes tadpole phenotypes to normalize prior to metamorphosis: prolactin hormone and *mmp* regulation.

The focus of this project, within the McLaughlin lab, can now be placed on discovering the exact roles that prolactin hormone and *mmp* gene regulation play in the process that leads to tissue remodeling after injury, and seeing whether there are other molecular factors involved in this unique mechanism. Specifically, performing RT-qPCR with cDNA from tadpoles that were not only exposed to one of the three chemical treatments, but also exposed to either PRL.2 or PM. Furthermore, the field of craniofacial research as well as the medical field could use the information gathered from this study to focus on developing non-surgical treatments for craniofacial deformities in humans, which is the goal of this thesis project.

Future directions

The most obvious future direction would be to continue to research *mmp* regulation in cDNA from the experimental groups after exposure to prolactin hormone though RT-qPCR procedure. This type of experiment could also show that the addition of PRL.2 helps in the normalization process of these tadpoles, which means supplemental prolactin hormone may be a better way to treat patients with CF deformities. The main goal is to elucidate the mechanism by which *Xenopus laevis* tadpoles self-correct CF abnormalities, but there are other important future directions that stem from the first two main experiments of this study.

The results of the study of the cerebrospinal fluid flow in malformed tadpole brains suggest that the abnormal brains hold the same amount of total CSF, but the overall brain size is smaller, resulting in hydrocephalus. According to the study by Hagenlocher et al., 2013, Hydrocephalus may result from overproduction of CSF and impaired reabsorption or obstruction of any of the ventricular ducts. The disorder leads to ventricle dilation and increased intracranial pressure. Loss of function of *foxj1* or absence of motile cilia can also cause hydrocephalus (Hagenlocher et al., 2013). Foxj1 is a key transcription factor that regulates the development of ependymal cell cilia (Miskevich, 2009). Thus, another future direction would be to test the function of the *foxj1* gene to see if loss of function is correlated with hydrocephalus in the treated tadpole brains (Hagenlocher et al., 2013). Confirming that *Xenopus laevis* pre-metamorphic tadpoles are exhibiting hydrocephalus in malformed brains, but can

self-correct, would have very large medical implications in treating hydrocephalus. Currently, the only way to treat hydrocephalus is to relieve the pressure in the brain through surgery (Miskevich, 2009).

Since the Pax7 protein expression pattern only exists in the midbrain and hindbrain, it would be effective to find a protein that shows a clear and consistent protein expression pattern in the forebrain to see if similar results are obtained. This is important to confirm whether the self-correction process is limited to certain regions of the brain or is specific to Pax7 expression only. We need to check to make sure the cell-level differentiation is normalized in all parts of the brain. Therefore, it would be helpful to run immunohistochemistry experiments for other proteins, such as the sonic hedgehog protein, which has been found to display a conserved protein spatial pattern in the *Xenopus laevis* larval forebrain (Domínguez et al., 2010).

Finally, an experiment to inhibit *prl.2* signaling in order to see whether self-correction would occur in malformed brains could confirm prolactin's direct involvement in the normalization of deformed brains over time. This could have large implications in creating novel treatments for craniofacial deformities in the future.

After addressing these future directions, we will have a better understanding of the ability of pre-metamorphic *Xenopus laevis* tadpoles to repair malformations in brain tissue, and we will be able to see whether the addition of PRL.2 causes a quicker normalization process among malformed brains. These

experimental proposals will help in the effort to discover the mechanism by which *Xenopus laevis* tadpoles fix their own craniofacial abnormalities, which would have huge implications in the medical field, and could allow us to treat human beings with common birth deformities in a more effective, less intrusive way than the surgical options that currently exist.

APPENDIX

Analyzing tyrosine hydroxylase protein expression patterns in pre-metamorphic *Xenopus laevis* brains

Introduction

Tyrosine hydroxylase plays a very important role in brain function. This protein is the rate-limiting enzyme of catecholamine biosynthesis (Daubner et al., 2011). Tyrosine hydroxylase changes tyrosine to L-DOPA, which then leads to the making of dopamine, norepinephrine, and epinephrine, all important hormones and neurotransmitters (Daubner et al., 2011). These neurotransmitters play a role in brain functions, such as attention, memory, cognition and emotion (Daubner et al., 2011). Non-functional tyrosine hydroxylase can have a great effect on the brain, causing the catecholamine biosynthesis pathway to be impaired (Daubner et al., 2011). In addition, there may be a link between this non-functioning protein and neurodegenerative diseases, such as Alzheimer's, Parkinson's and Huntington's disease (Daubner, et.al. 2011). We sought to utilize tyrosine hydroxylase as a marker for proper forebrain differentiation because based on previous research, it was predicted that the protein expression pattern would be seen in the forebrain, which cannot be determined with Pax7 (González et al., 1993).

I examined pre-metamorphic tadpoles that underwent one of three exposure treatments during neurogenesis: ICI 118,551 HCl, thioridazine HCl, or ethanol exposure. These treatments had been previously used in experiments in the McLaughlin lab, and were known to cause craniofacial deformities when tadpoles were exposed to the drugs during neurulation, stages 14-25 (Nieuwkoop & Faber, 1994). ICI 118,551 HCl is a β_2-adrenoceptor antagonist (Smith et al., 1987). Based on previous experiments done in the McLaughlin lab, ICI 118,551 HCl exposure during neurulation is known to cause abnormal trapezoidal-shaped head

phenotypes in tadpoles due to the absence of anterior mandibular cartilage elements. Thioridazine HCl is a dopamine receptor antagonist (Sachlos et al., 2012). Through previous experiments in the McLaughlin lab, it has been found to cause a square head phenotype, misshapen eyes, and hyper-pigmentation in tadpoles that were exposed to the drug during neurulation. Ethanol, a retinoic acid signaling antagonist, produces a very similar phenotype in tadpoles as a child with severe Fetal Alcohol Syndrome: microcephaly and ocular deformities (cone eyes) (Kot-Leibovich and Fainsod, 2009b; Shi et al., 2014). McLaughlin lab studies have also shown that the overall craniofacial morphology of the thioridazine HCl and ethanol treatment groups improve prior to metamorphosis, while the abnormal morphology of tadpoles in the ICI 118,551 HCl treatment group remain unchanged.

Since the results of the 2012 Vandenberg study revealed that tadpoles with craniofacial deformities were able to self-correct over time, we hypothesized that tadpoles with these defects may also show malformed brain tissue, and that this abnormal brain tissue would correct over time as well. I performed immunohistochemistry on control, ICI 118,551 HCl, thioridazine HCl, and ethanol tadpole brains using Tyrosine hydroxylase antibodies to analyze and score protein expression patterns in the brains of tadpoles at different pre-metamorphic stages, to determine whether the brain tissue in these treatment groups is properly differentiated. However, in the end, the high background signal in our immunohistochemistries reveal that tyrosine hydroxylase is far less of a specific brain region marker compared to Pax7.

Results

The tyrosine hydroxylase immunohistochemistries did not produce as clear of a protein expression pattern as that of the Pax7, as the normal expression shown by the control groups appeared to change slightly from stage to stage (Figure A.1). There was consistent expression in the hindbrain at each of the stages, especially along the ridges of the hindbrain. Stage 45 controls showed expression in the forebrain and the upper part of the midbrain in addition to the hindbrain, while stage 47 controls showed less expression in the forebrain (Figure A.1). Stage 49 controls had minimal expression in the forebrain (only at the very top of the brain) and the midbrain seemed to have slightly less than the stage before (Figure A.1). Finally, stage 50 controls showed most expression along the ridges of the hindbrain (Figure A.1).

In each of the stages examined (45, 47, 49 and 50) there seemed to be large differences in the percentage of abnormal tyrosine hydroxylase expression patterns between the treated groups and the control group (Figure A.2). For stage 45, 75% of the control brains had normal brain tyrosine hydroxylase expression patterning, 16.8% of brains had decreased expression, and 8.3% had increased expression (Figure A.2). The three treatment groups all had the same results: 40% of brains had normal expression, 40% of brains had decreased expression, and 20% of brains had increased expression (Figure A.2). There was also an extremely large difference between the percentage of brains with abnormal tissue in specimen exposed to ICI from stage 47 to 49 (100% abnormal to 20% abnormal expression) (Figure A.2).

Based on a single trial, by stage 50, the control group had 100% of brains with normal expression, while ICI and EtOH both had 25% of brains with normal expression. 25% of the ICI brains showed expanded expression, and 50% of brains showed ectopic expression in the midbrain. The EtOH brains showed 75% ectopic expression in the midbrain. The ThioHCl brains appeared to be much more similar to the controls, with 60% of the brains having normal expression and 40% of the brains having ectopic expression in the midbrain and forebrain.

Discussion

The results of the tyrosine hydroxylase immunohistochemistries showed that, similarly to Pax7, the treated groups at stage 45 all seemed to have abnormal expression patterns relative to controls. For this protein, it appeared that only the brains that had been exposed to ThioHCl were able to improve by stage 50 (Figure A.2). However, the stage 50 brain results come from only one trial, so the data could possibly be skewed, and more trials are needed to draw major conclusions. Another unexpected result was that there was not more of a consistent tyrosine hydroxylase expression pattern in the forebrain, as previous studies have reported (Domínguez et al., 2010; González et al., 1993). This issue might be resolved by adjusting concentrations of the antibody used or the timing of the chromogenic reaction in future trials.

Overall, this study seemed to show that brains which exhibited abnormal protein patterning at stage 45 were more likely to be able to show an improvement in Pax7 protein expression by stage 49/50 than tyrosine hydroxylase, which could

mean that the mid and hindbrain regions are better able to remodel and correct abnormal phenotypes. Also, it is possible that Pax7 is involved in the mechanism by which *Xenopus laevis* tadpoles reform damaged tissues prior to metamorphosis because the protein expression patterns seemed to improve as the overall morphology of the brain was improving.

In addition to further replicates of tyrosine hydroxylase immunohistochemistries, it may be helpful to do the immunohistochemistry experiment for other proteins such the sonic hedgehog protein (*x-Shh*) which has been found to express a largely conserved protein pattern in the *Xenopus laevis* forebrain (Domínguez et al., 2010). Due to the fact that tyrosine hydroxylase did not show a clear and consistent protein expression pattern in the forebrain, I would want to try to find a protein that does. The *x-Shh* protein is critical in the patterning of vertebrate embryonic tissues, including the brain and the spinal cord (Chiang et al., 1996). Defects in sonic hedgehog were found to cause cyclopia and absence of distal limbs, spinal column, and cells in the neural tube (Chiang et al., 1996).

Materials and Methods

Animal husbandry

Adult, female *Xenopus laevis* frogs were primed by injecting 0.75 mL of chorionic gonadotrophin hormone into their dorsal lymph sac in order to induce ovulation. The females were then placed in a 18°C incubator overnight in 4L buckets of frog water, each containing two frogs. After 16-18 hours, the frogs were gently squeezed to extract eggs, which were retrieved in a petri dish. The eggs were

then fertilized by a portion of a gonad, which had been surgically removed from a male *Xenopus laevis* frog after euthanasia. The gonads were stored at 4°C in 1X MBS (modified Barth's saline) solution. Zygotes were de-jellied with 2% cysteine and rinsed with 0.1X MMR (Marc's Modified Ringer's Solution: 1 M NaCl, 20 nM KCl, 10 nM $MgCl_2$, 20 nM $CaCl_2$, 50 mM HEPES), then placed in the 14°C incubator in fresh 0.1X MMR solution. As the embryos grew, dead or lysed embryos were removed, and the MMR solution was regularly changed.

Pharmaceutical exposures

Upon reaching stage 14 (approximately 48 hours after fertilization if kept at 14°C), the embryos were separated into four groups and exposed to different drugs. There was one control group, which was kept in 0.1X MMR, and three groups exposed to the following chemical treatments: 50 µM ICI 118, 551 in 0.1X MMR, 90 µM of thioridazine hydrochloride in 0.1X MMR, and 2% ethanol in 0.1X MMR. The tadpoles were exposed to these treatments only during neurulation; the exposure was stopped once the neural tube was completely formed at stage 26 (Nieuwkoop & Faber, 1994). After exposures during neurulation, the four groups were all switched to new petri dishes and reared in 0.1X MMR at 14°C until they reached the desired developmental stage.

Tadpole care and tissue preservation

The tadpoles were raised at 14°C until they reached stage 45-47, at which point the tadpoles were transferred to larger containers (Tupperware), kept at 22°C,

and fed three times a week with a Sera Micron mixture. When the tadpoles reached stage 45, approximately 25-30 tadpoles from each of the four groups were euthanized with tricaine (Fisher BioReagents), MEMFA-fixed (MEMFA: 10% 10X MEM salts, 10% formaldehyde, 80% Pico water), dehydrated in 100% methanol, and stored at -20°C. This MEMFA-fixing process was repeated when the tadpoles reached stages 47, 49, and 50. After fixation, the tadpoles were bleached with a 30% hydrogen peroxide and 70% methanol solution and exposed to a constant bright light overnight.

Immunohistochemistry

The bleached tadpoles were dissected to isolate the brains in preparation for whole mount immunohistochemistry (Caine and McLaughlin, 2013), with the following modifications: PBTr washes were cut down to half hour washes, only 1mL of the various antibody solutions were added to each of the wells containing brains, and the well-plate was rocked upright on a shaker at a low setting rather than a nutator. The tyrosine hydroxylase protein expression pattern was tested using the immunohistochemistry procedure. The tyrosine hydroxylase (diluted 1:40) (DSHB) antibody was derived from mice, so the secondary antibody used was goat anti-mouse AP (diluted 1/1500) (Sigma). Levamisole was added to the chromogenic reaction solution (100 nM Tris, 50 nM $MgCl_2$, 100 nM NaCl, 0.05% Tween-20, nitro blue tetrazolium [NBT] and 5-bromo-4-chloro-indolyl-phosphate [BCIP]) to reduce background staining.

The protein expression in the brains were scored as normal or abnormal, relative to the most consistent expression pattern of the control group. The abnormal patterns were further categorized into either expanded, decreased, or ectopic expression groups. 2-3 brains from each different exposure group and stage were imaged using a Nikon microscope and SPOT ImageSolutions™ software at 5X or 6X magnification.

Statistical analysis

Significant differences between the treatment and control groups, based on the quantitative scoring data, were calculated using a Chi-Square goodness of fit. The expected values in this analysis were the average control values for each stage, for only two categories: normal and abnormal protein expression patterns.

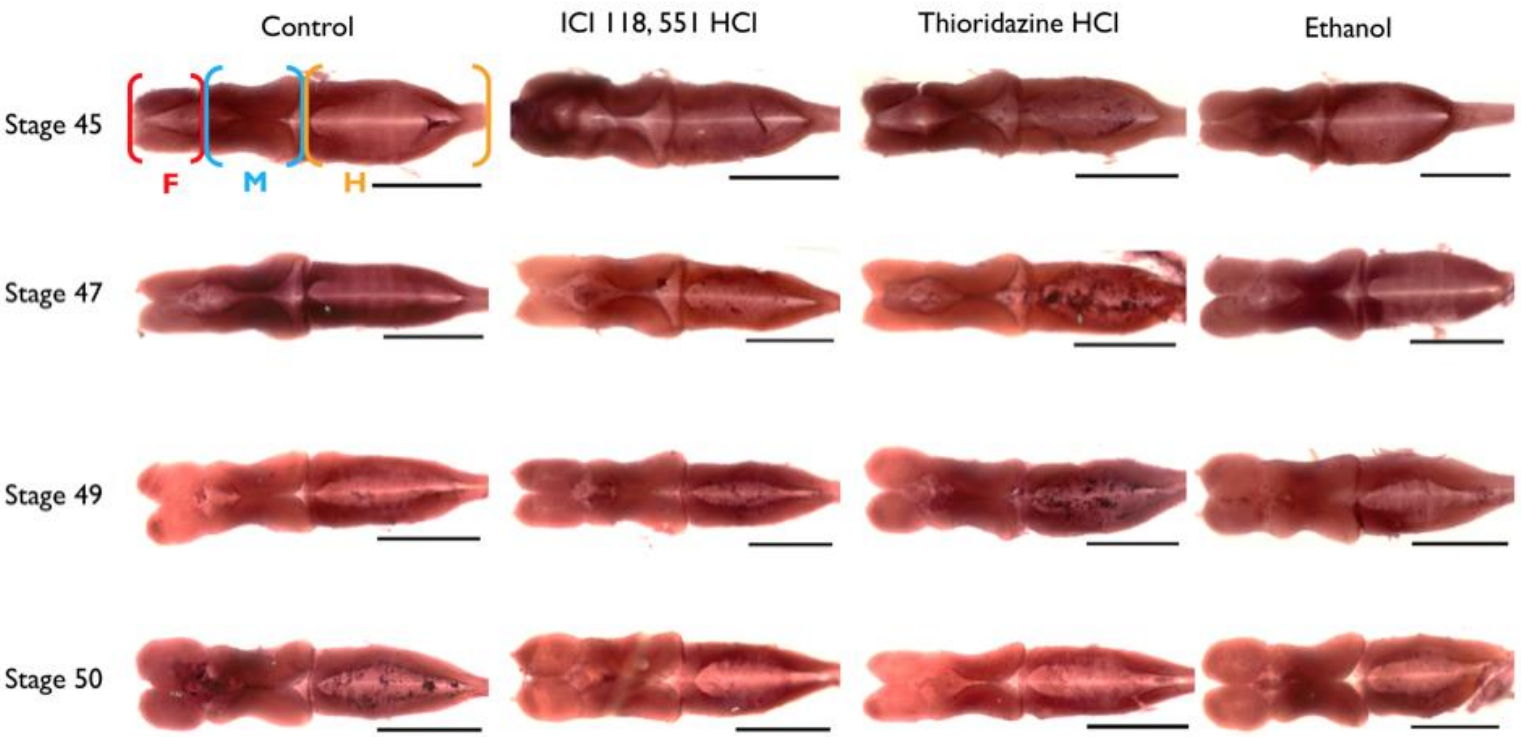

Figure A.1 Immunohistochemistry results showing tyrosine hydroxylase protein expression.

Figure A.1 Immunohistochemistry results showing tyrosine hydroxylase protein expression. Immunohistochemistry procedure was performed targeting tyrosine hydroxylase protein expression in the brains of control, ICI 118,551 HCl, thioridazine HCl, and ethanol-exposed pre-metamorphic *Xenopus laevis* tadpoles at NF stages 45, 47, 49 and 50. It appears that many areas of the brain may express tyrosine hydroxylase, as a clear protein expression pattern was not attained. From stage 45 to stage 50, it appears that the brains are normalizing, but it's hard to say if the brains are improving, or if the tyrosine hydroxylase gene is just dynamic. Scale bar = 500μm.

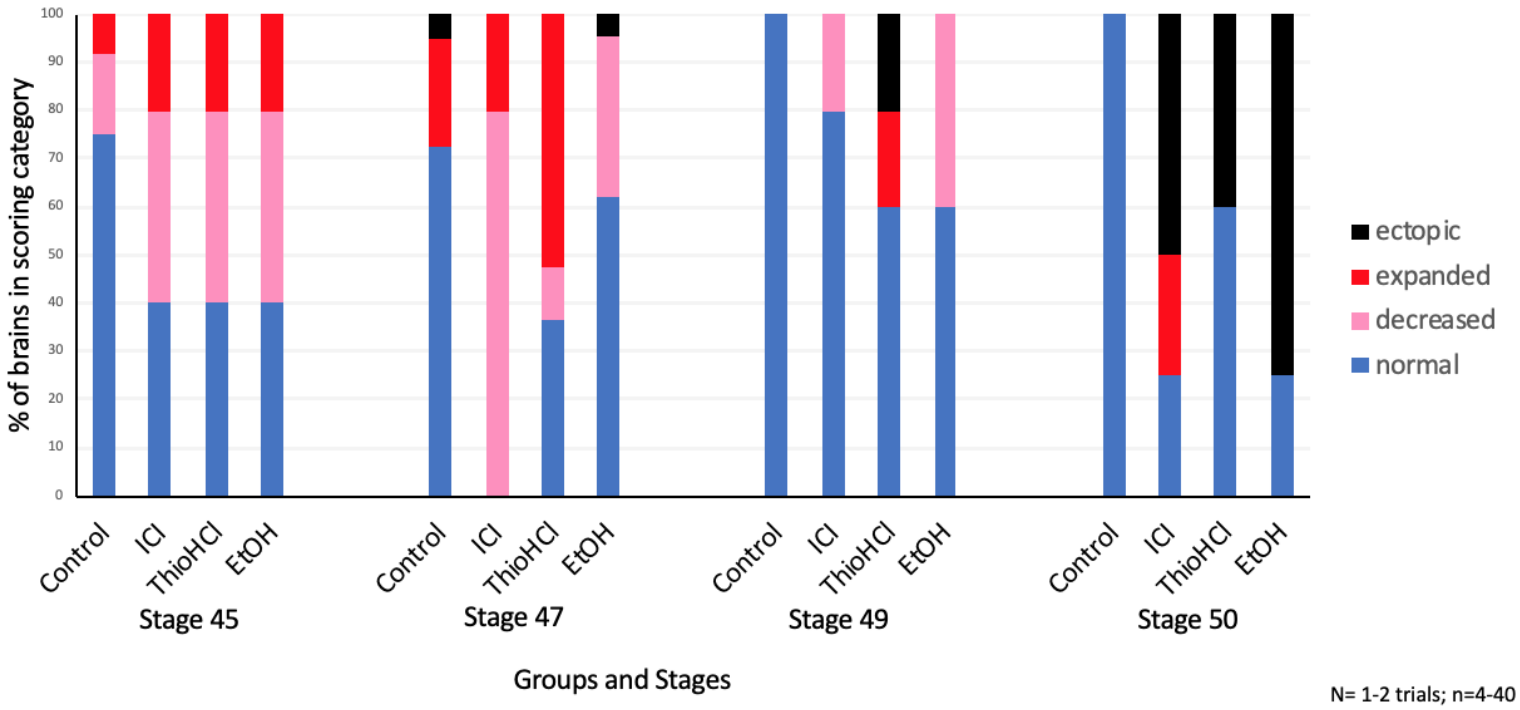

Figure A.2Scoring results of the tyrosine hydroxylase protein expression.

Figure A.2 Scoring results of the tyrosine hydroxylase protein expression. Each brain was scored as normal or abnormal basing the normal pattern on the control group for each individual stage. The abnormal brains were then categorized as showing either ectopic, decreased, or expanded expression. The bar graph shows the percentage of brains in each scoring category, so the bars add to 100%. As can be seen in the legend, blue is normal expression, red is expanded expression, pink is decreased expression, and black is ectopic expression. Treatment groups appear abnormal at stage 45. Improvement is seen in the thioridazine HCl group, but not in the other treatment groups. N=2 trials for control stage 45, and control, ThioHCl and EtOH for stage 47; N=1 trial for every other group; n=19-40 tadpole brains per group per stage for control stage 45, and control, ThioHCl and EtOH stage 47; n=4-5 tadpole brains per group per stage for every other group.

REFERENCES

ACHILLEOS, A. & TRAINOR, P. A. 2015. Chapter Sixteen - Mouse Models of Rare Craniofacial Disorders. *In:* YANG, C. (ed.) *Current Topics in Developmental Biology.* Academic Press.

ADAMEYKO, I. & FRIED, K. 2016. The Nervous System Orchestrates and Integrates Craniofacial Development: A Review. *Frontiers in Physiology,* 7**,** 49.

BAAS, D., MEINIEL, A., BENADIBA, C., BONNAFE, E., MEINIEL, O., REITH, W. & DURAND, B. 2006. A deficiency in RFX3 causes hydrocephalus associated with abnormal differentiation of ependymal cells. *Eur J Neurosci,* 24.

BANDÍN, S., MORONA, R., LÓPEZ, J. M., MORENO, N. & GONZÁLEZ, A. 2014. Immunohistochemical analysis of Pax6 and Pax7 expression in the CNS of adult Xenopus laevis. *Journal of Chemical Neuroanatomy,* 57-58**,** 24-41.

BANDÍN, S., MORONA, R., MORENO, N. & GONZÁLEZ, A. 2013. Regional expression of Pax7 in the brain of Xenopus laevis during embryonic and larval development. *Frontiers in Neuroanatomy,* 7.

BANIZS, B., PIKE, M. M., MILLICAN, C. L., FERGUSON, W. B., KOMLOSI, P., SHEETZ, J., BELL, P. D., SCHWIEBERT, E. M. & YODER, B. K. 2005. Dysfunctional cilia lead to altered ependyma and choroid plexus function, and result in the formation of hydrocephalus. *Development,* 132.

BEURDEN, P. A. M. S.-V. & HOFF, J. W. V. D. 2005. Zymographic techniques for the analysis of matrix metalloproteinases and their inhibitors. *BioTechniques,* 38**,** 73-83.

BILOTTA, J., BARNETT, J. A., HANCOCK, L. & SASZIK, S. 2004. Ethanol exposure alters zebrafish development: a novel model of fetal alcohol syndrome. *Neurotoxicol Teratol,* 26**,** 737-43.

BLACKISTON, D. J. & LEVIN, M. 2012. Aversive Training Methods in Xenopus laevis: General Principles. *Cold Spring Harbor protocols,* 2012**,** 10.1101/pdb.top068338 pdb.top068338.

BLACKISTON, D. J. & LEVIN, M. 2013. Ectopic eyes outside the head in Xenopus tadpoles provide sensory data for light-mediated learning. *J Exp Biol,* 216**,** 1031-40.

BROWN, D. D. 1995. The thyroid hormone-induced tail resorption program during Xenopus laevis metamorphosis. *Proc Natl Acad Sci U S A,* 93**,** 1924-1929.

CAINE, S. T. & MCLAUGHLIN, K. A. 2013. Regeneration of Functional Pronephric Proximal Tubules After Partial Nephrectomy in Xenopus laevis. *Developmental Dynamics,* 242**,** 219-229.

CAMPANTICO, E., GIUNTA, C., GUARDABASSI, A. & VIETTI, M. 1972. The stabilizing action of prolactin on the lysosomes in tails from Xenopus laevis daudin tadpoles. *General and Comparative Endocrinology,* 18**,** 396-399.

CARPETA, S., PINEDA, T., MARTÍNEZ, M. C., OSORIO, G., PORRAS-HURTADO, G. L., ROJAS, J., ZARANTE, I. & MORENO-NIÑO, O. M. 2018. 22q11.2 Deletion Syndrome in Colombian Patients With Syndromic Cleft Lip and/or Palate. *The Cleft Palate-Craniofacial Journal*, 1055665618770307.

CARVAN, M. J., 3RD, LOUCKS, E., WEBER, D. N. & WILLIAMS, F. E. 2004. Ethanol effects on the developing zebrafish: neurobehavior and skeletal morphogenesis. *Neurotoxicol Teratol,* 26**,** 757-68.

CHIANG, C., LITINGTUNG, Y., LEE, E., YOUNG, K. E., CORDEN, J. L., WESTPHAL, H. & BEACHY, P. A. 1996. Cyclopia and defective axial patterning in mice lacking Sonic hedgehog gene function. *Nature,* 383**,** 407.

CHIANG, W. W., TAKOUDIS, C. G., LEE, S. H., WEIS-MCNULTY, A., GLICK, R. & ALPERIN, N. 2009. Relationship between ventricular morphology and aqueductal cerebrospinal fluid flow in healthy and communicating hydrocephalus. *Invest Radiol,* 44.

CHRISTENSEN, K. E., BAHOUS, R. H., HOU, W., DENG, L., MALYSHEVA, O. V., ARNING, E., BOTTIGLIERI, T., CAUDILL, M. A., JEROME-MAJEWSKA, L. A. & ROZEN, R. 2018. Low Dietary Folate Interacts with MTHFD1 Synthetase Deficiency in Mice, a Model for the R653Q Variant, to Increase Incidence of Developmental Delays and Defects. *The Journal of Nutrition,* 148**,** 501-509.

CLOUTHIER, DAVID E., WILLIAMS, S.CLAY, YANAGISAWA, HIROMI, WIEDUWILT, MATTHEW, RICHARDSON, JAMES A., &YANAGISAWA, MASASHI. (2000). Signaling Pathways Crucial for Craniofacial Development Revealed by Endothelin-A Receptor-Deficient Mice. *Developmental Biology, 217*(1), 10-24.

COSTANZA, M. & PEDOTTI, R. 2016. Prolactin: Friend or Foe in Central Nervous System Autoimmune Inflammation? *International journal of molecular sciences,* 17**,** 2026.

DAUBNER, S. C., LE, T. & WANG, S. 2011. Tyrosine Hydroxylase and Regulation of Dopamine Synthesis. *Archives of biochemistry and biophysics,* 508**,** 1-12.

DOMÍNGUEZ, L., GONZÁLEZ, A. & MORENO, N. 2010. Sonic hedgehog expression during Xenopus laevis forebrain development. *Brain Research,* 1347**,** 19-32.

DUBEY, A. & SAINT-JEANNET, J.-P. 2017. Modeling human craniofacial disorders in Xenopus. *Current pathobiology reports,* 5**,** 79-92.

FACTOR, S. A. 1999. DOPAMINE AGONISTS. *Medical Clinics of North America,* 83**,** 415-443.

FEDERICO MARINI, J. M., HARALD BINDER 2015. flowcatchR: A framework for tracking and analyzing flowing blood cells in time lapse microscopy images. *Conference Proceeding*.

FITZGERALD, P. & DINAN, T. G. 2008. Prolactin and dopamine: What is the connection? A Review Article. *Journal of Psychopharmacology,* 22**,** 12-19.

FRISTON, K., LEVIN, M., SENGUPTA, B. & PEZZULO, G. 2015. Knowing one's place: a free-energy approach to pattern regulation. *J R Soc Interface,* 12.

FU, L., DAS, B., MATHEW, S. & SHI, Y.-B. 2009. Genome-wide identification of Xenopus matrix metalloproteinases: conservation and unique duplications in amphibians. *BMC Genomics,* 10**,** 81-81.

GAETE, M., MUÑOZ, R., SÁNCHEZ, N., TAMPE, R., MORENO, M., CONTRERAS, E. G., LEE-LIU, D. & LARRAÍN, J. 2012. Spinal cord regeneration in Xenopus tadpoles proceeds through activation of Sox2-positive cells. *Neural Dev,* 7.

GONZÁLEZ, A., TUINHOF, R. & SMEETS, W. J. A. J. 1993. Distribution of tyrosine hydroxylase and dopamine immunoreactivities in the brain of the South African clawed frog Xenopus laevis. *Anatomy and Embryology,* 187**,** 193-201.

GOODWIN, A. F., KIM, R., BUSH, J. O. & KLEIN, O. D. 2015. Chapter Seventeen - From Bench to Bedside and Back: Improving Diagnosis and Treatment of Craniofacial Malformations Utilizing Animal Models. *In:* YANG, C. (ed.) *Current Topics in Developmental Biology.* Academic Press.

GREGG, C., SHIKAR, V., LARSEN, P., MAK, G., CHOJNACKI, A., YONG, V. W. & WEISS, S. 2007. White Matter Plasticity and Enhanced Remyelination in the Maternal CNS. *The Journal of Neuroscience,* 27**,** 1812-1823.

GUIZZETTI, M. 2015. Chapter 3 - Fetal Alcohol Spectrum Disorders: Effects and Mechanisms of Ethanol on the Developing Brain A2 - Aschner, Michael. *In:* COSTA, L. G. (ed.) *Environmental Factors in Neurodevelopmental and Neurodegenerative Disorders.* Boston: Academic Press.

HAGENLOCHER, C., WALENTEK, P., MÜLLER, C., THUMBERGER, T. & FEISTEL, K. 2013. Ciliogenesis and cerebrospinal fluid flow in the developing Xenopus brain are regulated by foxj1. *Cilia,* 2**,** 12.

HEIMEIER, R. A., DAS, B., BUCHHOLZ, D. R., FIORENTINO, M. & SHI, Y.-B. 2010. Studies on Xenopus laevisintestine reveal biological pathways underlying vertebrate gut adaptation from embryo to adult. *Genome Biology,* 11**,** R55.

HERRERA-RINCON, C. & LEVIN, M. 2018. Booting up the organism during development: Pre-behavioral functions of the vertebrate brain in guiding body morphogenesis. *Communicative & Integrative Biology,* 11**,** e1433440.

HU, D., YOUNG, N. M., XU, Q., JAMNICZKY, H., GREEN, R. M., MIO, W., MARCUCIO, R. S. & HALLGRIMSSON, B. 2015. Signals from the brain induce variation in avian facial shape. *Dev Dyn*.

HUANG, H. & BROWN, D. D. 2000a. Overexpression of Xenopus laevis growth hormone stimulates growth of tadpoles and frogs. *Proceedings of the National Academy of Sciences of the United States of America,* 97**,** 190-194.

HUANG, H. & BROWN, D. D. 2000b. Prolactin is not a juvenile hormone in Xenopus laevis metamorphosis. *Proceedings of the National Academy of Sciences,* 97**,** 195-199.

HUANG, X., HUI, M. N. Y., LIU, Y., YUEN, D. S. H., ZHANG, Y., CHAN, W. Y., LIN, H. R., CHENG, S. H. & CHENG, C. H. K. 2009. Discovery of a Novel Prolactin in Non-Mammalian Vertebrates: Evolutionary Perspectives and Its Involvement in Teleost Retina Development. *PLOS ONE,* 4**,** e6163.

IBAÑEZ-TALLON, I., PAGENSTECHER, A., FLIEGAUF, M., OLBRICH, H., KISPERT, A., KETELSEN, U. P., NORTH, A., HEINTZ, N. & OMRAN, H. 2004. Dysfunction of axonemal dynein heavy chain Mdnah5 inhibits ependymal flow and reveals a novel mechanism for hydrocephalus formation. *Hum Mol Genet,* 13.

JABŁOŃSKA-TRYPUĆ, A., MATEJCZYK, M. & ROSOCHACKI, S. 2016. Matrix metalloproteinases (MMPs), the main extracellular matrix (ECM) enzymes in collagen degradation, as a target for anticancer drugs. *Journal of Enzyme Inhibition and Medicinal Chemistry,* 31**,** 177-183.

JOVEN, A., MORONA, R., GONZÁLEZ, A. & MORENO, N. 2013. Spatiotemporal Patterns of Pax3, Pax6, and Pax7 Expression in the Developing Brain of a Urodele Amphibian, Pleurodeles waltl. *Journal of Comparative Neurology,* 521**,** 3913-3953.

JUNG, J.-C., WEST-MAYS, J. A., STRAMER, B. M., BYRNE, M. H., SCOTT, S., MODY, M. K., SADOW, P. M., KRANE, S. M. & FINI, M. E. 2004. Activity and expression of Xenopus laevis matrix metalloproteinases: Identification of a novel role for the hormone prolactin in regulating collagenolysis in both amphibians and mammals. *Journal of Cellular Physiology,* 201**,** 155-164.

KODITUWAKKU, P. & KODITUWAKKU, E. 2014. Cognitive and Behavioral Profiles of Children with Fetal Alcohol Spectrum Disorders. *Current Developmental Disorders Reports,* 1**,** 149-160.

KOT-LEIBOVICH, H. & FAINSOD, A. 2009a. Ethanol induces embryonic malformations by competing for retinaldehyde dehydrogenase activity during vertebrate gastrulation. *Dis Model Mech,* 2**,** 295-305.

KOT-LEIBOVICH, H. & FAINSOD, A. 2009b. Ethanol induces embryonic malformations by competing for retinaldehyde dehydrogenase activity during vertebrate gastrulation. *Disease Models & Mechanisms,* 2**,** 295-305.

KUMAR, A., SINGH, C. K., DIPETTE, D. D. & SINGH, U. S. 2010. Ethanol impairs activation of retinoic acid receptors in cerebellar granule cells in a rodent model of fetal alcohol spectrum disorders. *Alcohol Clin Exp Res,* 34**,** 928-37.

LIU, K. J. 2016. Animal models of craniofacial anomalies. *Dev Biol,* 415**,** 169-170.

LOVE, M. I., HUBER, W. & ANDERS, S. 2014. Moderated estimation of fold change and dispersion for RNA-seq data with DESeq2. *Genome Biology,* 15**,** 550.

MAEDA, S., SAWAI, T., UZUKI, M., TAKAHASHI, Y., OMOTO, H., SEKI, M. & SAKURAI, M. 1995. Determination of interstitial collagenase (MMP-1) in patients with rheumatoid arthritis. *Annals of the rheumatic diseases,* 54**,** 970-975.

MARCUCIO, R., HALLGRIMSSON, B. & YOUNG, N. M. 2015. Chapter Twelve - Facial Morphogenesis: Physical and Molecular Interactions Between the Brain and the Face. *In:* CHAI, Y. (ed.) *Current Topics in Developmental Biology.* Academic Press.

MARRS, J. A., CLENDENON, S. G., RATCLIFFE, D. R., FIELDING, S. M., LIU, Q. & BOSRON, W. F. 2010. Zebrafish fetal alcohol syndrome model: effects of ethanol are rescued by retinoic acid supplement. *Alcohol,* 44**,** 707-15.

MOGI, K., ADACHI, T., IZUMI, S. & TOYOIZUMI, R. 2012. Visualisation of cerebrospinal fluid flow patterns in albino Xenopus larvae in vivo. *Fluids and Barriers of the CNS,* 9**,** 9.

MORENO, N., JOVEN, A., MORONA, R., BANDÍN, S., LÓPEZ, J. M. & GONZÁLEZ, A. 2014. Conserved localization of Pax6 and Pax7 transcripts in the brain of representatives of sarcopterygian vertebrates during development supports homologous brain regionalization. *Frontiers in neuroanatomy,* 8**,** 75-75.

MISKEVICH, F. (2010). Imaging fluid flow and cilia beating pattern in Xenopus brain ventricles. *Journal of Neuroscience Methods, 189*(1), 1-4.

NAITOH, H., SUGANUMA, Y., UEDA, Y., SATO, T., HIRAMUKI, Y., FUJISAWA-SEHARA, A., TAKETANI, S. & ARAKI, M. 2017. Upregulation of matrix metalloproteinase triggers transdifferentiation of retinal pigmented epithelial cells in Xenopus laevis: A Link between inflammatory response and regeneration. *Developmental Neurobiology,* 77**,** 1086-1100.

P.D. NIEUWKOOP AND J. FABER, E. 1994. *Normal table of Xenopus laevis (daudin),* New York, NY, Routledge.

PAI, V. P., PIETAK, A., WILLOCQ, V., YE, B., SHI, N.-Q. & LEVIN, M. 2018. HCN2 Rescues brain defects by enforcing endogenous voltage pre-patterns. *Nature Communications,* 9**,** 998.

PARHAR, I. S. 2003. Gonadotropin-releasing hormone receptors: neuroendocrine regulators and neuromodulators. *Fish Physiology and Biochemistry,* 28**,** 13-18.

PARKER, SAMANTHA E., CARA T. MAI, MARK A. CANFIELD, RUSSEL RICKARD, YING WANG, ROBERT E. MEYER, PATRICK ANDERSON, CRAIG A. MANSON, JULIANNE S. COLLINS, RUSSEL S. KIRBY, & ADOLFO CORREA. "Updated National Birth Prevalence Estimates for Selected Birth Defects in the United States, 2004–2006." *Birth Defects Research Part A: Clinical and Molecular Teratology* 88, no. 12 (2010): 1008-016.

PATEL, N., KHAN, A. O., ALSAHLI, S., ABDEL-SALAM, G., NOWILATY, S. R., MANSOUR, A. M., NABIL, A., AL-OWAIN, M., SOGATI, S., SALIH, M. A., KAMAL, A. M., ALSHARIF, H., ALSAIF, H. S.,

ALZAHRANI, S. S., ABDULWAHAB, F., IBRAHIM, N., HASHEM, M., FAQUIH, T., SHAH, Z. A., ABOUELHODA, M., MONIES, D., DASOUKI, M., SHAHEEN, R., WAKIL, S. M., ALDAHMESH, M. A. & ALKURAYA, F. S. 2018. Genetic investigation of 93 families with microphthalmia or posterior microphthalmos. *Clinical Genetics,* 93**,** 1210-1222.

PÉREZ-FÍGARES, J. M., JIMENEZ, A. J. & RODRÍGUEZ, E. M. 2001. Subcommissural organ, cerebrospinal fluid circulation, and hydrocephalus. *Microsc Res Tech,* 52.

PHILIPS, N. & MCFADDEN, K. 2004. Inhibition of transforming growth factor-beta and matrix metalloproteinases by estrogen and prolactin in breast cancer cells. *Cancer Letters,* 206**,** 63-68.

PINET, K. J. (2019). The adaptive remodeling and repair mechanisms responsible for the correction of malformed craniofacial and brain tissue in pre-metamorphic *Xenopus laevis*.

QUILLARD, T., ARAÚJO, H. A., FRANCK, G., TESMENITSKY, Y. & LIBBY, P. 2014. Matrix metalloproteinase-13 predominates over matrix metalloproteinase-8 as the functional interstitial collagenase in mouse atheromata. *Arteriosclerosis, thrombosis, and vascular biology,* 34**,** 1179-1186.

REID, N., HARNETT, P., O'CALLAGHAN, F., SHELTON, D., WYLLIE, M. & DAWE, S. 2018. Physiological self-regulation and mindfulness in children with a diagnosis of fetal alcohol spectrum disorder. *Developmental Neurorehabilitation***,** 1-6.

ROBERTS, R. M., MATHIAS, J. L. & WHEATON, P. 2012. Cognitive Functioning in Children and Adults With Nonsyndromal Cleft Lip and/or Palate: A Meta-analysis. *Journal of Pediatric Psychology,* 37**,** 786-797.

SACHLOS, E., RISUEÑO, RUTH M., LARONDE, S., SHAPOVALOVA, Z., LEE, J.-H., RUSSELL, J., MALIG, M., MCNICOL, JAMIE D., FIEBIG-COMYN, A., GRAHAM, M., LEVADOUX-MARTIN, M., LEE, JUNG B., GIACOMELLI, ANDREW O., HASSELL, JOHN A., FISCHER-RUSSELL, D., TRUS, MICHAEL R., FOLEY, R., LEBER, B., XENOCOSTAS, A., BROWN, ERIC D., COLLINS, TONY J. & BHATIA, M. 2012. Identification of Drugs Including a Dopamine Receptor Antagonist that Selectively Target Cancer Stem Cells. *Cell,* 149**,** 1284-1297.

SCHINDELIN, J., ARGANDA-CARRERAS, I., FRISE, E., KAYNIG, V., LONGAIR, M., PIETZSCH, T., PREIBISCH, S., RUEDEN, C., SAALFELD, S., SCHMID, B., TINEVEZ, J. Y., WHITE, D. J., HARTENSTEIN, V., ELICEIRI, K., TOMANCAK, P. & CARDONA, A. 2012. Fiji: an open-source platform for biological-image analysis. *Nat Methods,* 9.

SCHREIBER, A. M., DAS, B., HUANG, H., MARSH-ARMSTRONG, N. & BROWN, D. D. 2001. Diverse developmental programs of Xenopus laevis metamorphosis are inhibited by a dominant negative thyroid hormone

receptor. *Proceedings of the National Academy of Sciences,* 98**,** 10739-10744.

SESSION, A. M., UNO, Y., KWON, T., CHAPMAN, J. A., TOYODA, A., TAKAHASHI, S., FUKUI, A., HIKOSAKA, A., SUZUKI, A., KONDO, M., VAN HEERINGEN, S. J., QUIGLEY, I., HEINZ, S., OGINO, H., OCHI, H., HELLSTEN, U., LYONS, J. B., SIMAKOV, O., PUTNAM, N., STITES, J., KUROKI, Y., TANAKA, T., MICHIUE, T., WATANABE, M., BOGDANOVIC, O., LISTER, R., GEORGIOU, G., PARANJPE, S. S., VAN KRUIJSBERGEN, I., SHU, S., CARLSON, J., KINOSHITA, T., OHTA, Y., MAWARIBUCHI, S., JENKINS, J., GRIMWOOD, J., SCHMUTZ, J., MITROS, T., MOZAFFARI, S. V., SUZUKI, Y., HARAMOTO, Y., YAMAMOTO, T. S., TAKAGI, C., HEALD, R., MILLER, K., HAUDENSCHILD, C., KITZMAN, J., NAKAYAMA, T., IZUTSU, Y., ROBERT, J., FORTRIEDE, J., BURNS, K., LOTAY, V., KARIMI, K., YASUOKA, Y., DICHMANN, D. S., FLAJNIK, M. F., HOUSTON, D. W., SHENDURE, J., DUPASQUIER, L., VIZE, P. D., ZORN, A. M., ITO, M., MARCOTTE, E. M., WALLINGFORD, J. B., ITO, Y., ASASHIMA, M., UENO, N., MATSUDA, Y., VEENSTRA, G. J. C., FUJIYAMA, A., HARLAND, R. M., TAIRA, M. & ROKHSAR, D. S. 2016. Genome evolution in the allotetraploid frog Xenopus laevis. *Nature,* 538**,** 336.

SHI, Y., LI, J., CHEN, C., GONG, M., CHEN, Y., LIU, Y., CHEN, J., LI, T. & SONG, W. 2014. 5-mehtyltetrahydrofolate rescues alcohol-induced neural crest cell migration abnormalities. *Molecular Brain,* 7**,** 67.

SHINGO, T., GREGG, C., ENWERE, E., FUJIKAWA, H., HASSAM, R., GEARY, C., CROSS, J. C. & WEISS, S. 2003. Pregnancy-Stimulated Neurogenesis in the Adult Female Forebrain Mediated by Prolactin. *Science,* 299**,** 117-120.

SIMOES-COSTA, M. & BRONNER, M. E. 2015. Establishing neural crest identity: a gene regulatory recipe. *Development,* 142**,** 242-57.

SMITH, G. W., HALL, J. C., FARMER, J. B. & SIMPSON, W. T. 1987. The cardiovascular actions of dopexamine hydrochloride, an agonist at dopamine receptors and β2-adrenoceptors in the dog. *Journal of Pharmacy and Pharmacology,* 39**,** 636-641.

SONG, I. & DITYATEV, A. 2018. Crosstalk between glia, extracellular matrix and neurons. *Brain Research Bulletin,* 136**,** 101-108.

SQUARE, T., JANDZIK, D., CATTELL, M., COE, A., DOHERTY, J. & MEDEIROS, D. M. 2015. A gene expression map of the larval Xenopus laevis head reveals developmental changes underlying the evolution of new skeletal elements. *Developmental Biology,* 397**,** 293-304.

STAVELEY, D. B. E. (2019). Vertebrate Development I: Life Cycles and Experimental Techniques. Retrieved from http://www.mun.ca/biology/desmid/brian/BIOL3530/DEVO_03/

UEDA, A. I.-O. A. S. 1996. Apoptosis and cell proliferation in *Xenopus* small intestine during meramorphosis. *Cell & Tissue Research,* 286**,** 467-476.

VAN OTTERLOO, E., CORNELL, R. A., MEDEIROS, D. M. & GARNETT, A. T. 2013. Gene regulatory evolution and the origin of macroevolutionary novelties: insights from the neural crest. *Genesis (New York, N.Y. : 2000),* 51**,** 457-470.

VAN OTTERLOO, E., WILLIAMS, T. & ARTINGER, K. B. 2016. The old and new face of craniofacial research: How animal models inform human craniofacial genetic and clinical data. *Developmental Biology,* 415**,** 171-187.

VANDENBERG, MORRIE, & ADAMS. (2011). V-ATPase-dependent ectodermal voltage and pH regionalization are required for Xenopus craniofacial morphogenesis. *Developmental Biology, 356*(1), 148.

VANDENBERG, L. N., ADAMS, D. S. & LEVIN, M. 2012. Normalized shape and location of perturbed craniofacial structures in the Xenopus tadpole reveal an innate ability to achieve correct morphology. *Dev Dyn,* 241**,** 863-78.

VEENING JAN G, & BARENDREGT HENK P. (2010). The regulation of brain states by neuroactive substances distributed via the cerebrospinal fluid; a review. *Cerebrospinal Fluid Research, 7*(1), 1.

VISSE, R. & NAGASE, H. 2003. Matrix Metalloproteinases and Tissue Inhibitors of Metalloproteinases. *Structure, Function, and Biochemistry,* 92**,** 827-839.

WEBSTER, W. S., WALSH, D. A., MCEWEN, S. E. & LIPSON, A. H. 1983. Some teratogenic properties of ethanol and acetaldehyde in C57BL/6J mice: Implications for the study of the fetal alcohol syndrome. *Teratology,* 27**,** 231-243.

YELIN, R., KOT, H., YELIN, D. & FAINSOD, A. 2007. Early molecular effects of ethanol during vertebrate embryogenesis. *Differentiation,* 75**,** 393-403.

YUEH, T.-C., WU, C.-N., HUNG, Y.-W., CHANG, W.-S., FU, C.-K., PEI, J.-S., WU, M.-H., LAI, Y.-L., LEE, Y.-M., YEN, S.-T., LI, H.-T., TSAI, C.-W. & BAU, D. A. T. 2018. The Contribution of MMP-7 Genotypes to Colorectal Cancer Susceptibility in Taiwan. *Cancer genomics & proteomics,* 15**,** 207-212.

ZHORNITSKY, S., WEE YONG, V., KOCH, M. W., MACKIE, A., POTVIN, S., PATTEN, S. B. & METZ, L. M. 2013. Quetiapine Fumarate for the Treatment of Multiple Sclerosis: Focus on Myelin Repair. *CNS Neuroscience & Therapeutics,* 19**,** 737-744.